
超新星遗迹物理
和X射线辐射
南京大学 陈阳
2025-08-22 昆明

“客星”：历史超新星

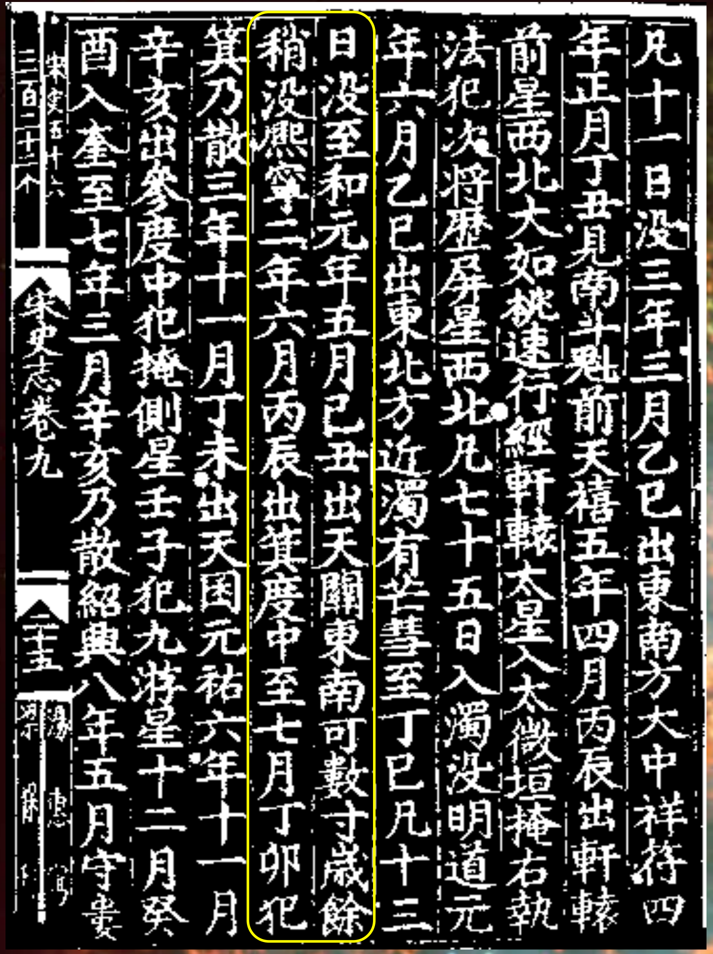

凡十一日沒三年三月乙巳出東南方大中祥符四
年正月丁丑見南斗魁前天禧五年四月丙辰出軒轅
前星西北大如桃速行經軒轅太星入太微垣掩右執
法犯次將歷屏星西北凡七十五日入濁沒明道元
年六月乙巳出東北方近濁有芒彗至丁巳凡十三
日沒至和元年五月己丑出天關東南可數寸歲餘
稍沒熙寧二年六月丙辰出箕度中至七月丁卯犯
箕乃散三年十一月丁未出天囷元祐六年十一月
辛亥出參度中犯掩側星壬子犯九游星十二月癸
酉入奎至七年三月辛亥乃散紹興八年五月守婁

宋史志卷九

1054年中国北宋天文学家发现金牛座“客星”（超新星）

《宋史．天文志》：

（宋）至和元年五月己丑（1054年7月4日），（客星）出天关东南可数寸，岁余稍没。

《宋会要》：

嘉祐元年（1056年）三月，司天監言：客星没，客去之兆也。初，至和元年（1054年）五月，**晨出東方，守天關，昼見如太白，芒角四出，色赤白，凡見二十三日。**

第谷（Tycho），AD1572（11月）

453周年

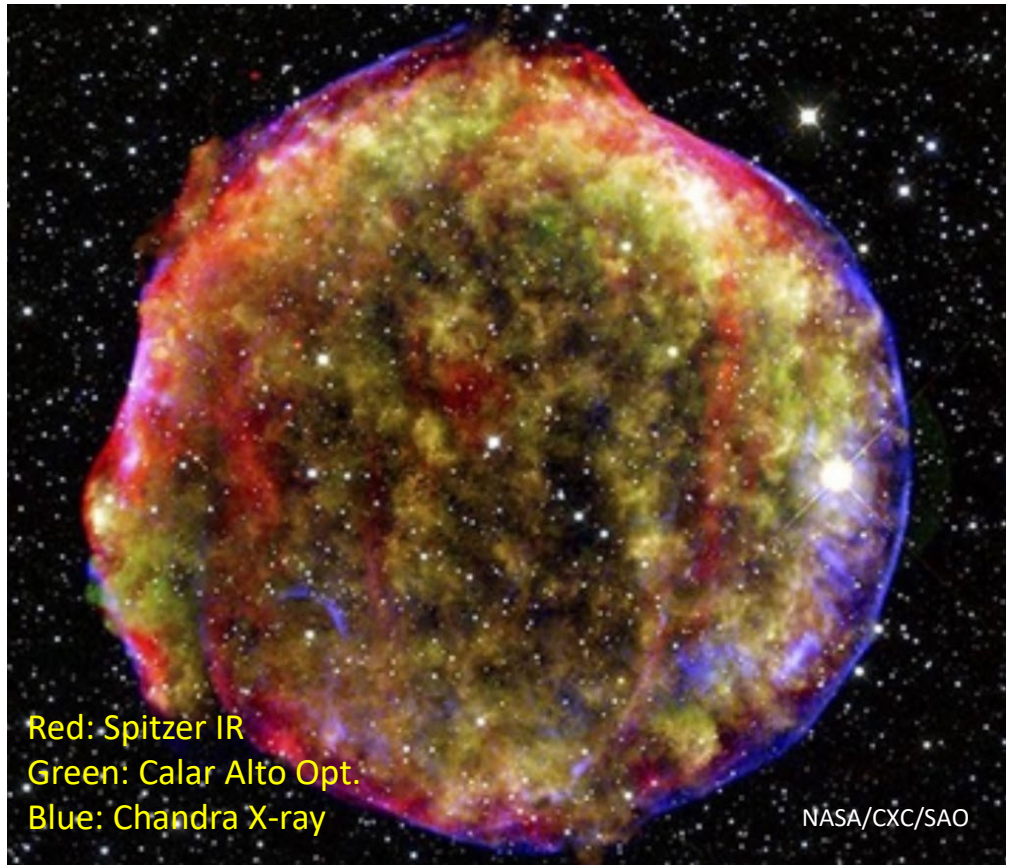

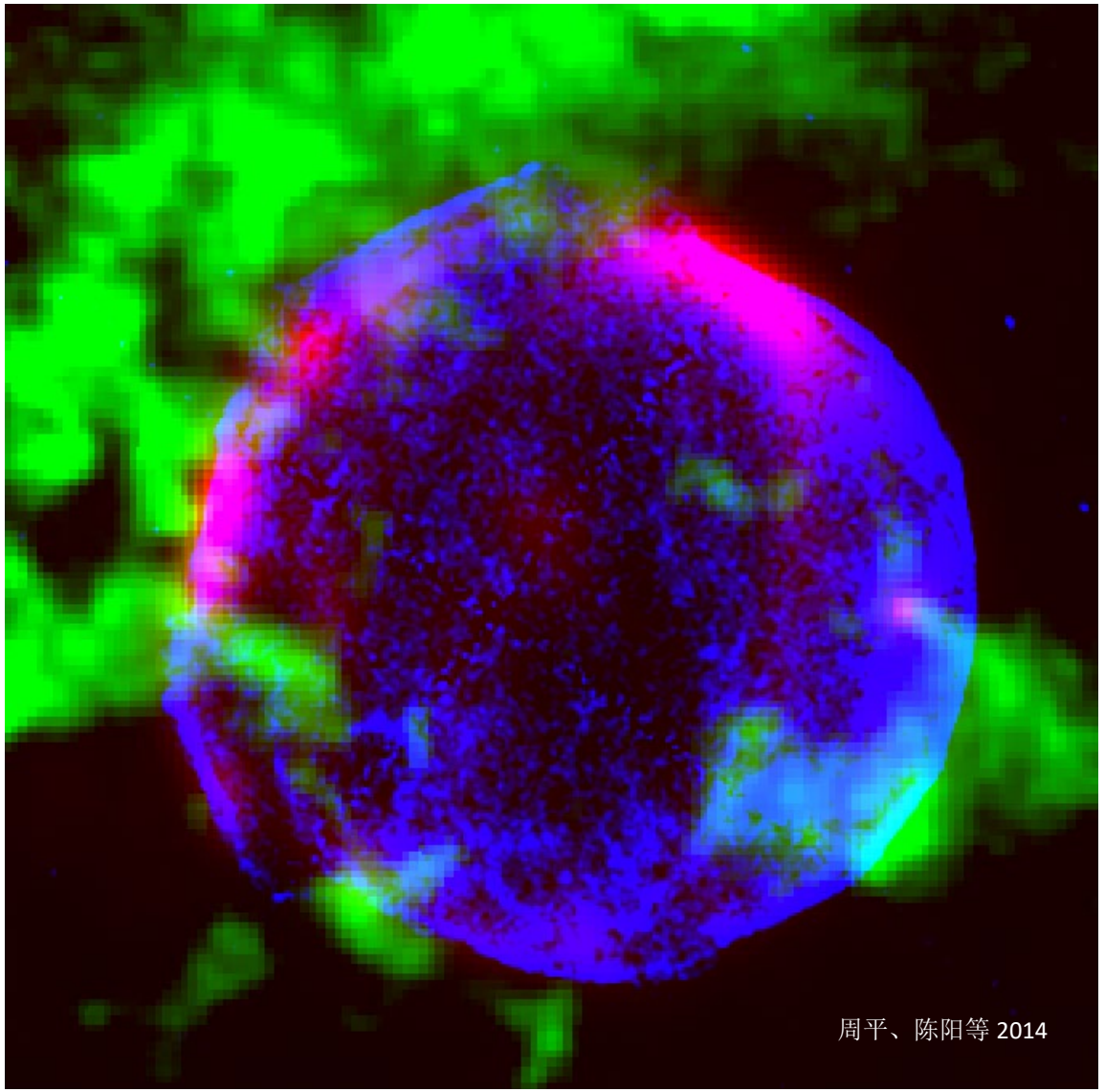

http://heasarc.gsfc.nasa.gov/docs/objects/heapow/archive/nebulae/sn1987a_acis.html

超新星1987A

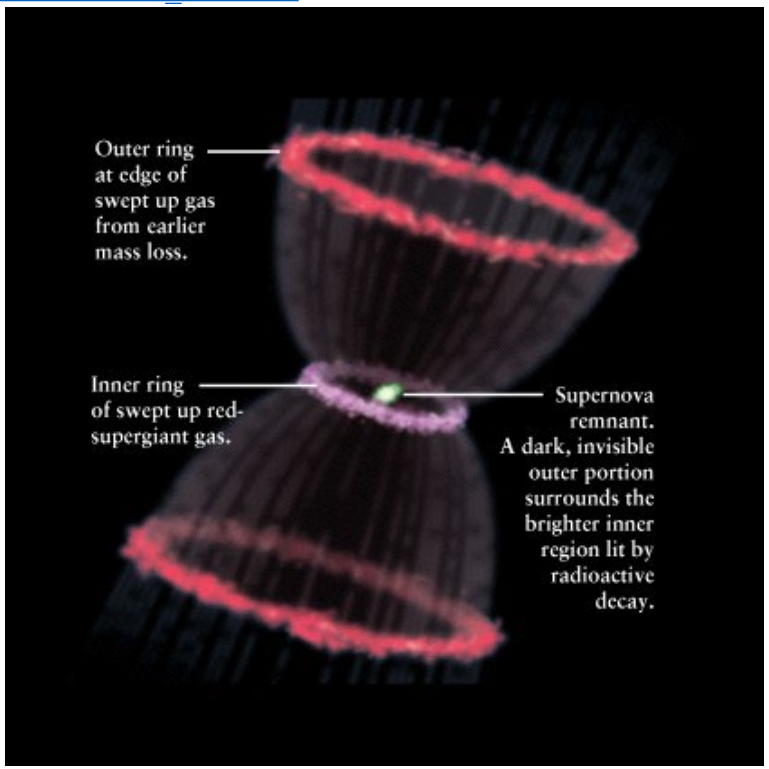

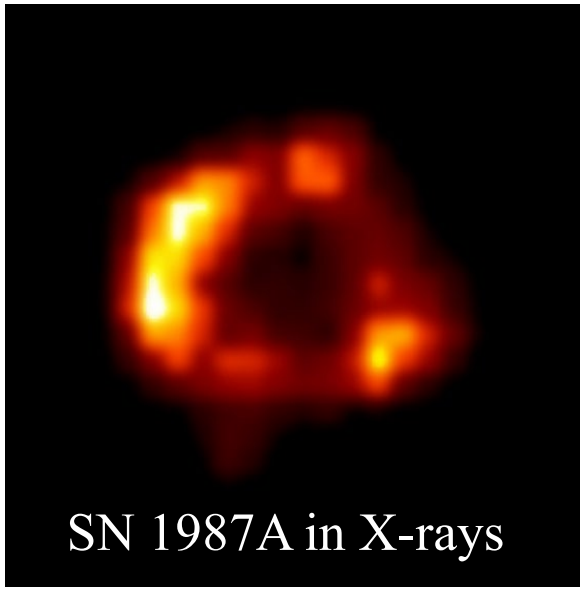

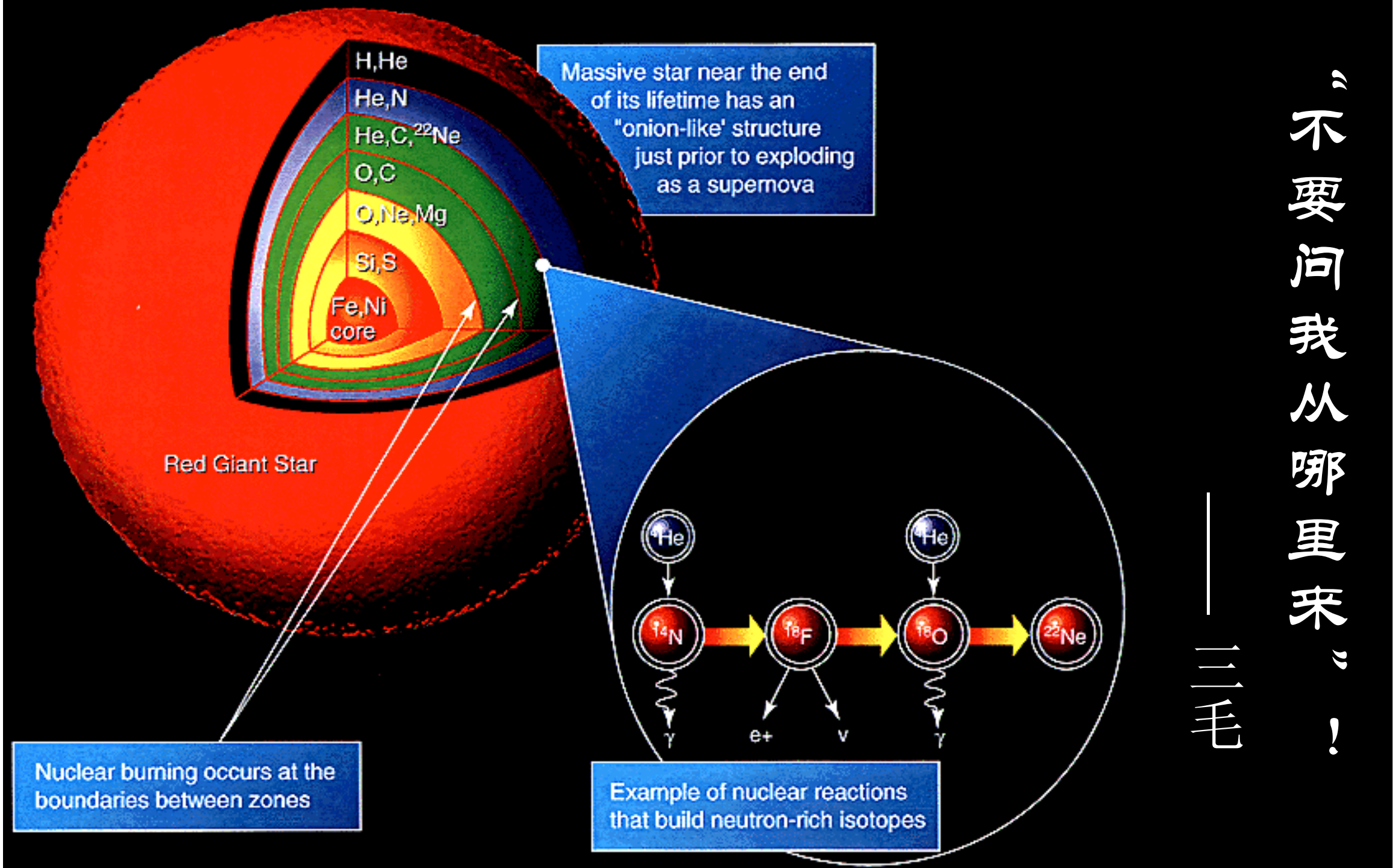
H,He
He,N
He,C,22Ne
O,C
O,Ne,Mg
Si,S
Fe,Ni core
Red Giant Star
Massive star near the end of its lifetime has an "onion-like' structure just prior to exploding as a supernova
Nuclear burning occurs at the boundaries between zones
4He
14N
18F
18O
22Ne
4He
γ
e+
ν
γ
Example of nuclear reactions that build neutron-rich isotopes

“不要问我从哪里来，”

——三毛

Classification of SNe

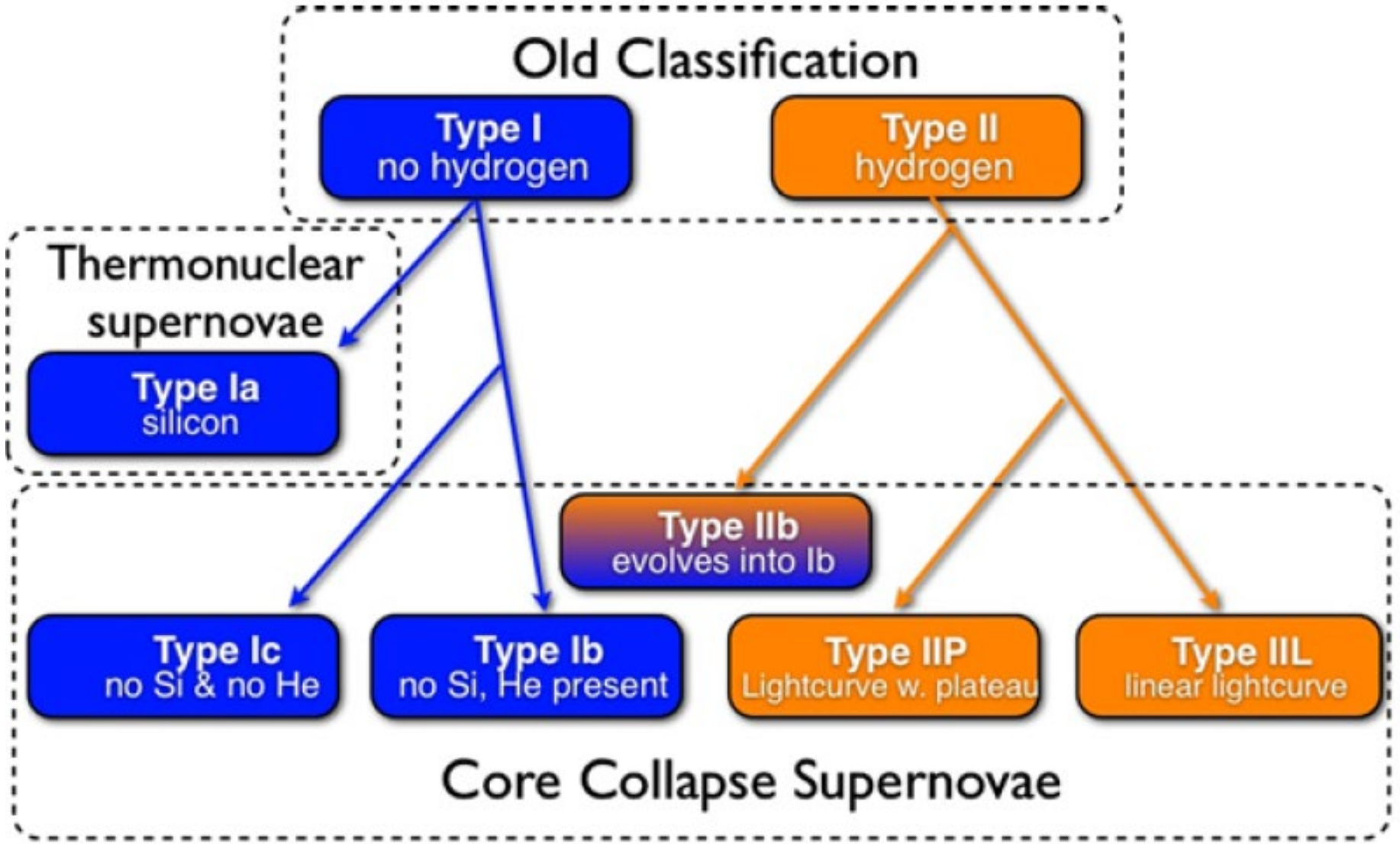

Classification of SNRs

Galactic：~300

Magellanic：~80

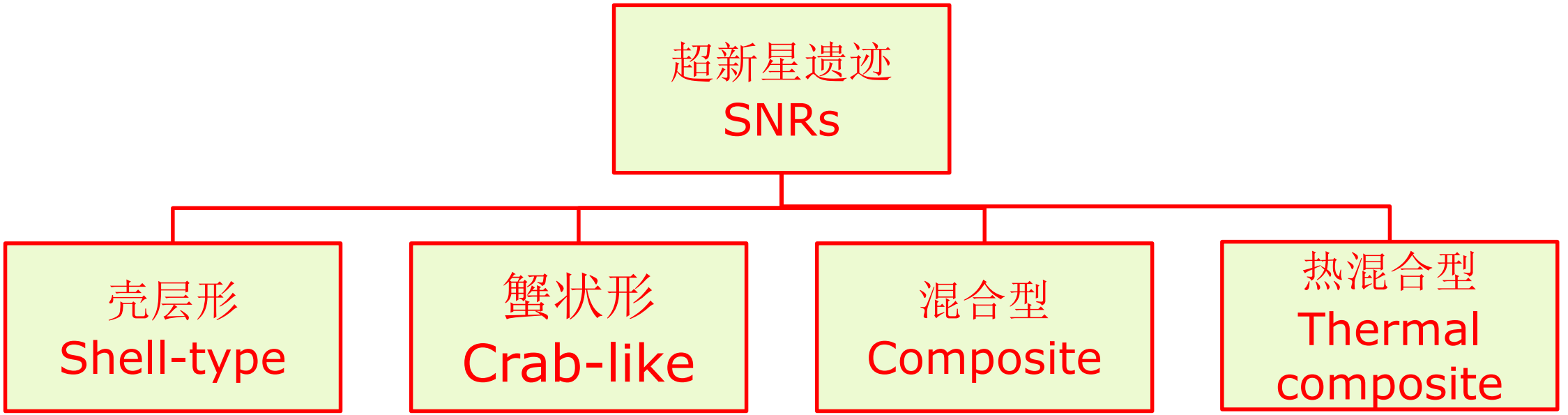

or: Mixed-morphplogy

Shell-type SNRs

SN1006

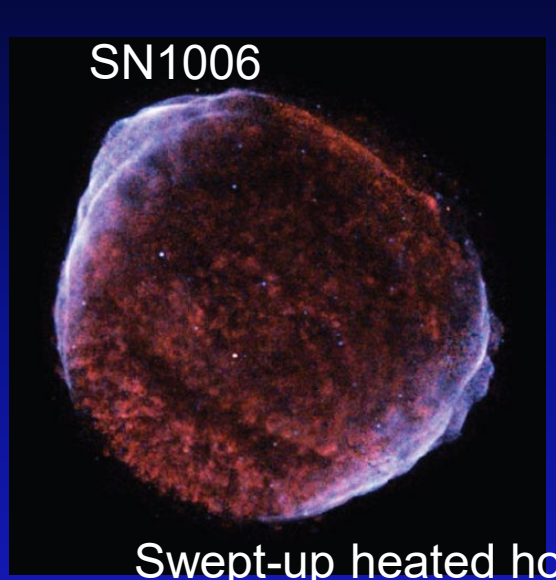

Kepler

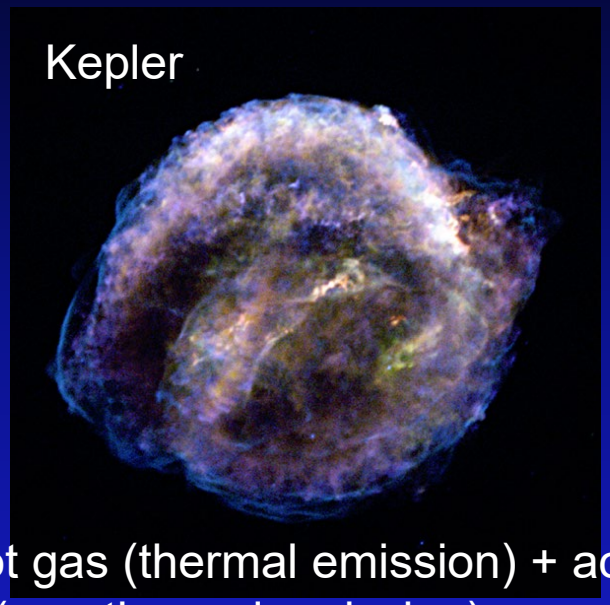

N132D （萧潇 & 陈阳 2007）

Swept-up heated hot gas (thermal emission) + accelerated relativistic particles (non-thermal emission)

Tycho

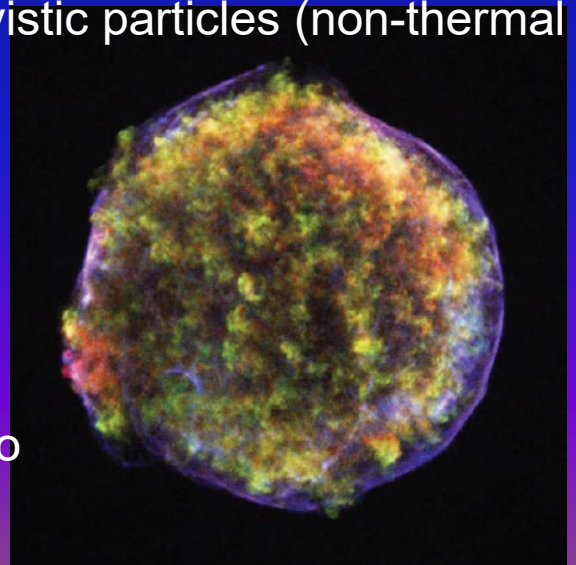

Cas A

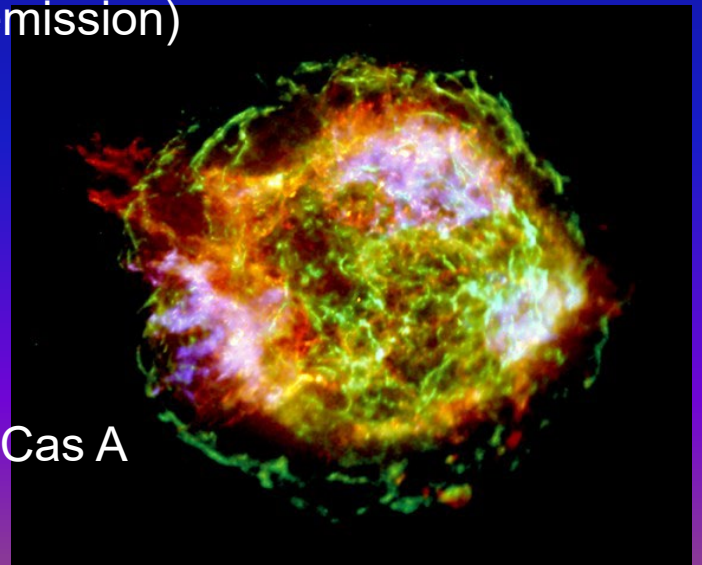

Crab-like SNRs

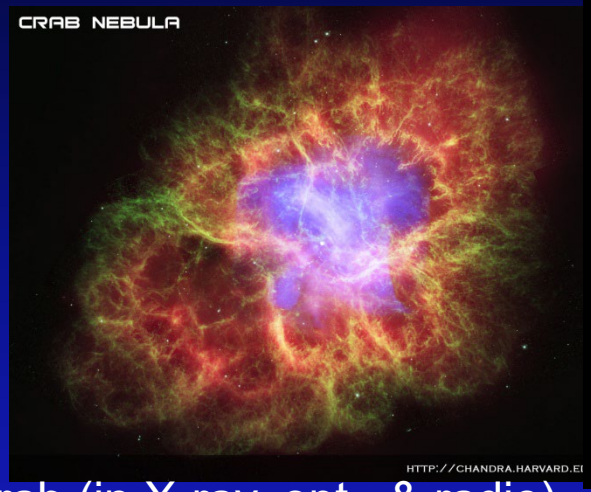

Crab (in X-ray, opt., & radio)

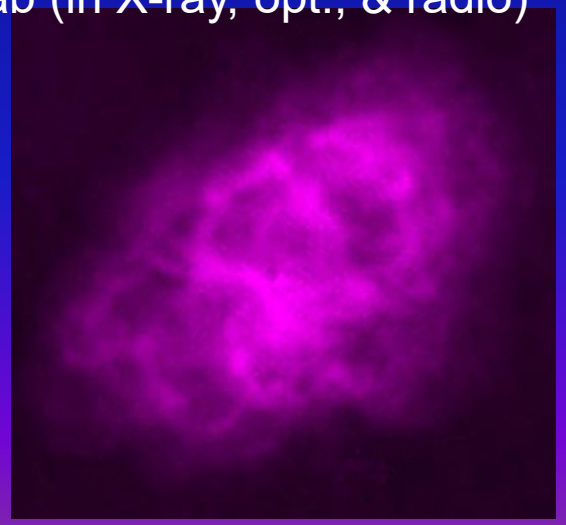

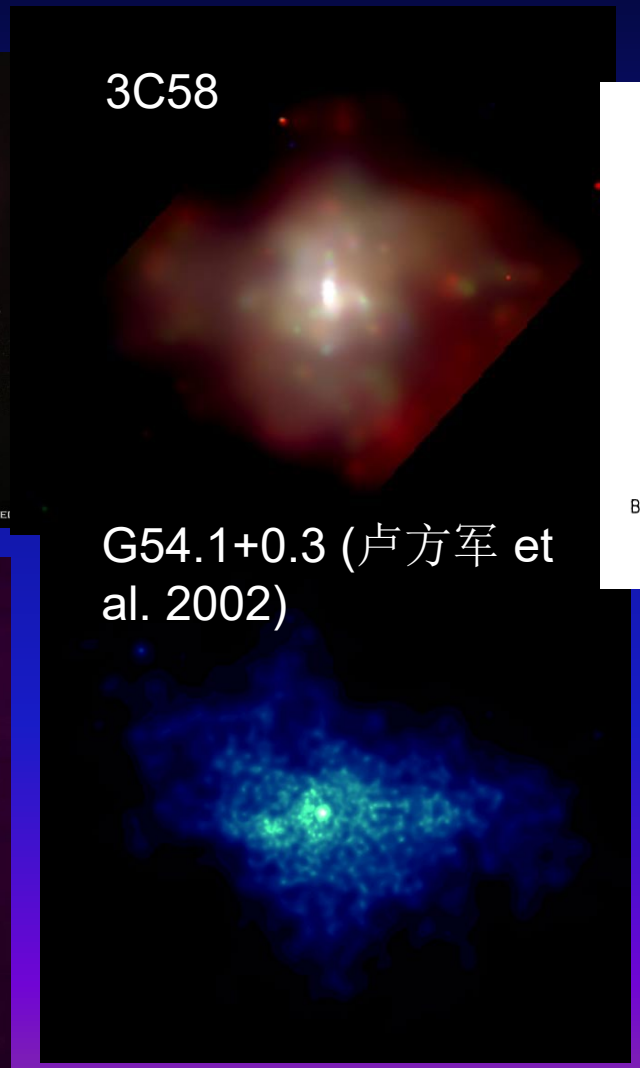

G54.1+0.3 (卢方军 et al. 2002)

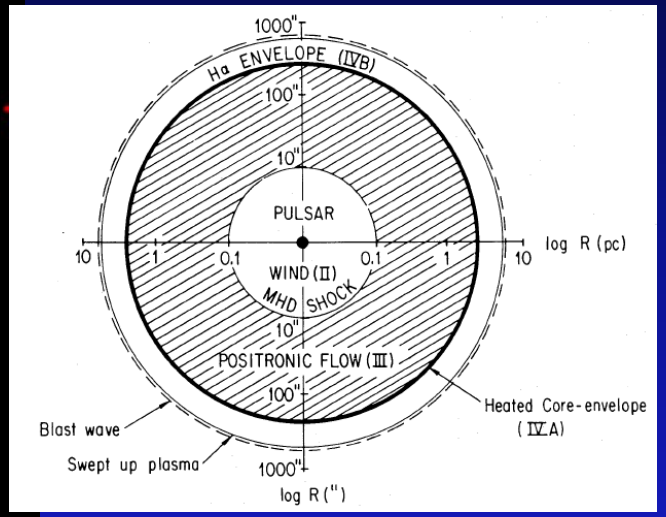

Pulsars, left by the core-collapse SN explosion, power the relativistic winds – pulsar wind nebulae (PWNe)

Composite SNRs

G11.2–0.3

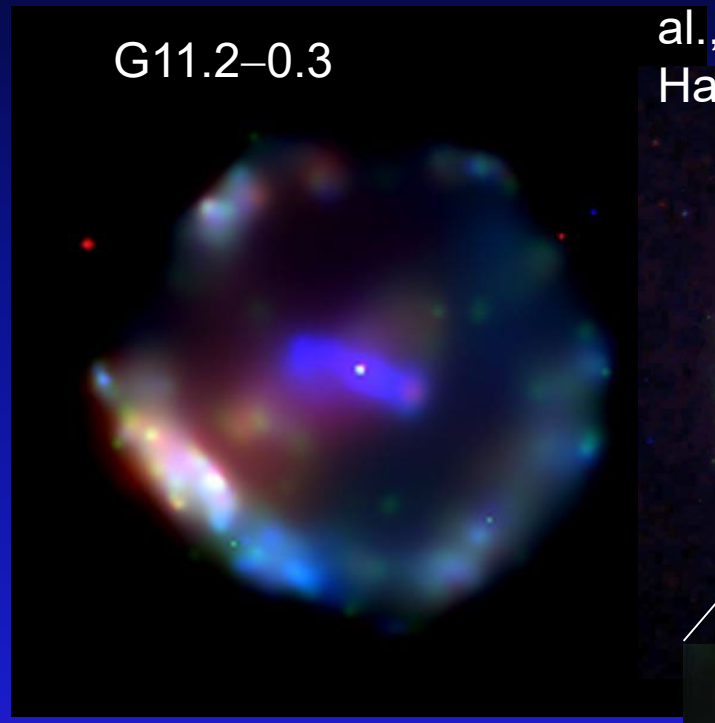

G21.5–0.9 (Slane & 陈阳 et al., 2001; Metheson & Safi-Harb 2005)

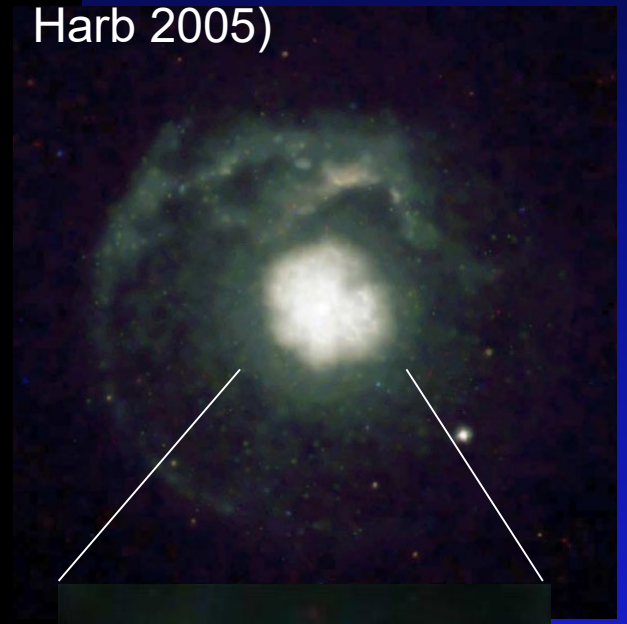

N157B (陈阳, 王青德, et al., 2006)

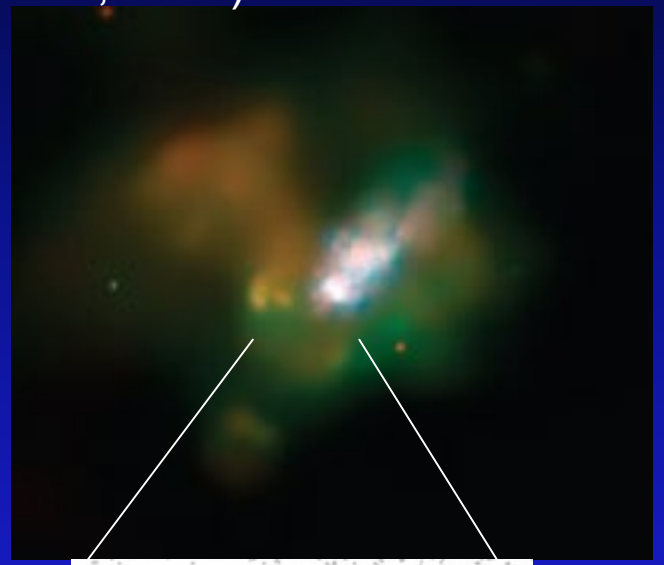

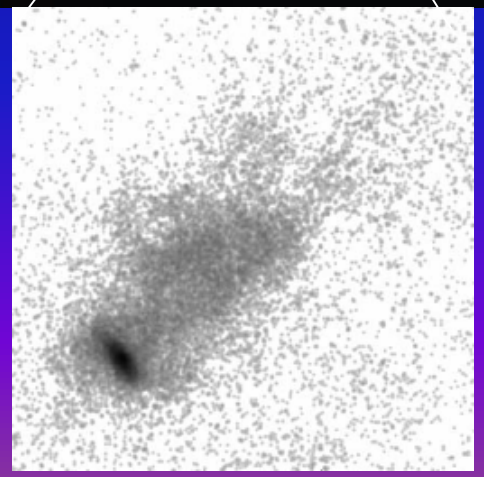

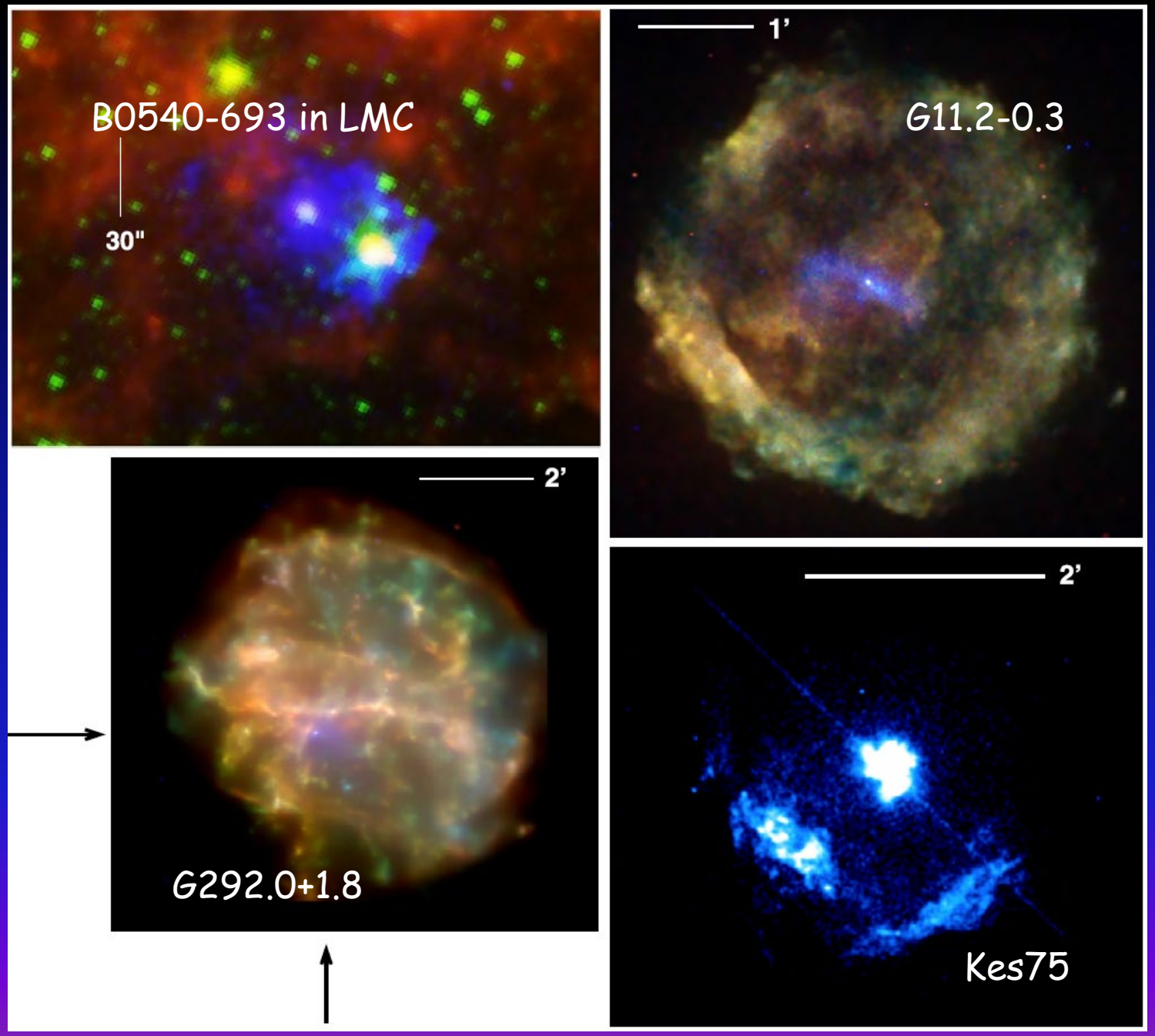

Reynolds 2017, SSR

Thermal Composite (TC) (Mixed morphology)

- Radio shell (blastwave)
- Associated with MCs (but not all)

  often with OH Masers

  (signpost of shock interaction with MCs)
- Interior thermal X-rays, some with $T_z > T_e$

  intriguing, nature *UNCLEAR* !

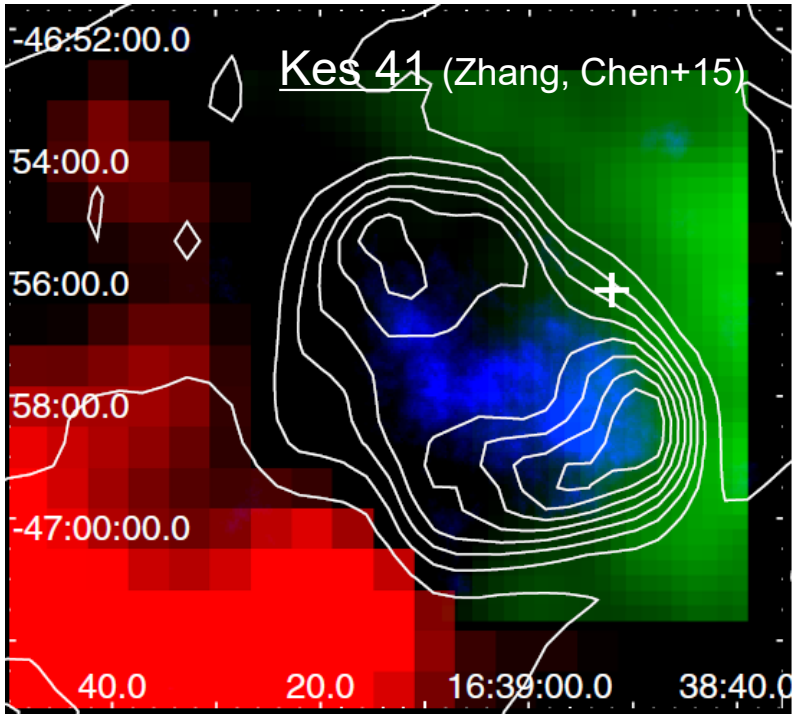

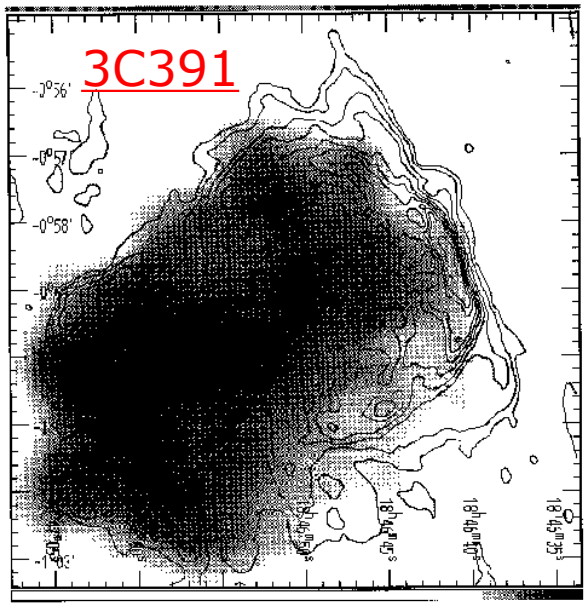

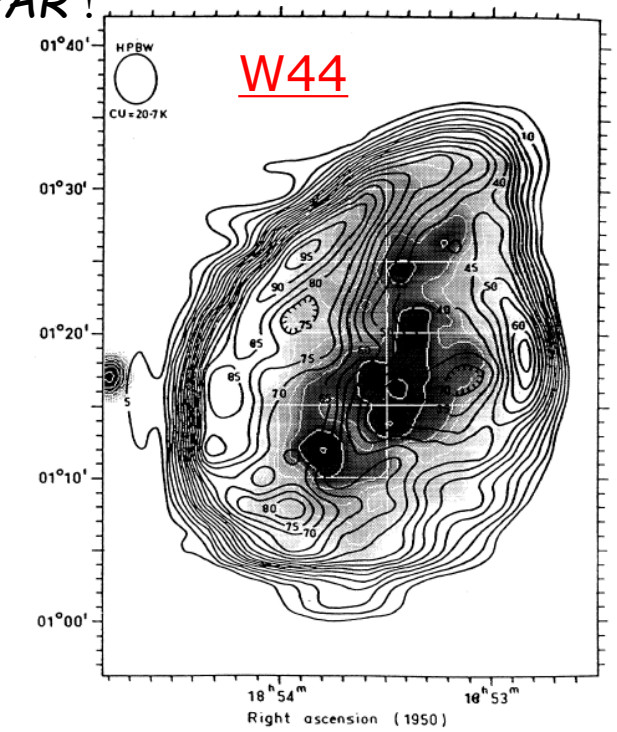

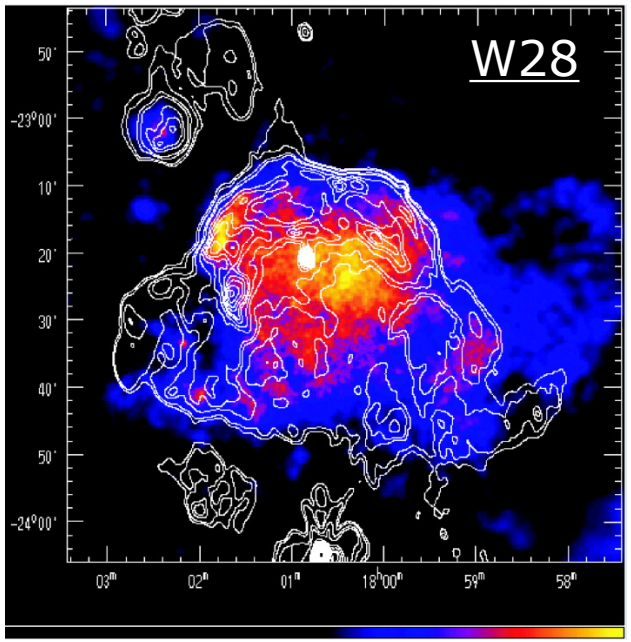

超新星（遗迹）爆震波的演化

Type Ia SNe: 14%
Core-collapse (> $8M_{\odot}$) : 86%

Isotropic explosion and further evolution
Homogeneous ambient medium
Three phases:

- Free expansion
- Adiabatic expansion
- Radiative expansion

超新星（遗迹）爆震波：自由膨胀相

Forward and reverse shocks

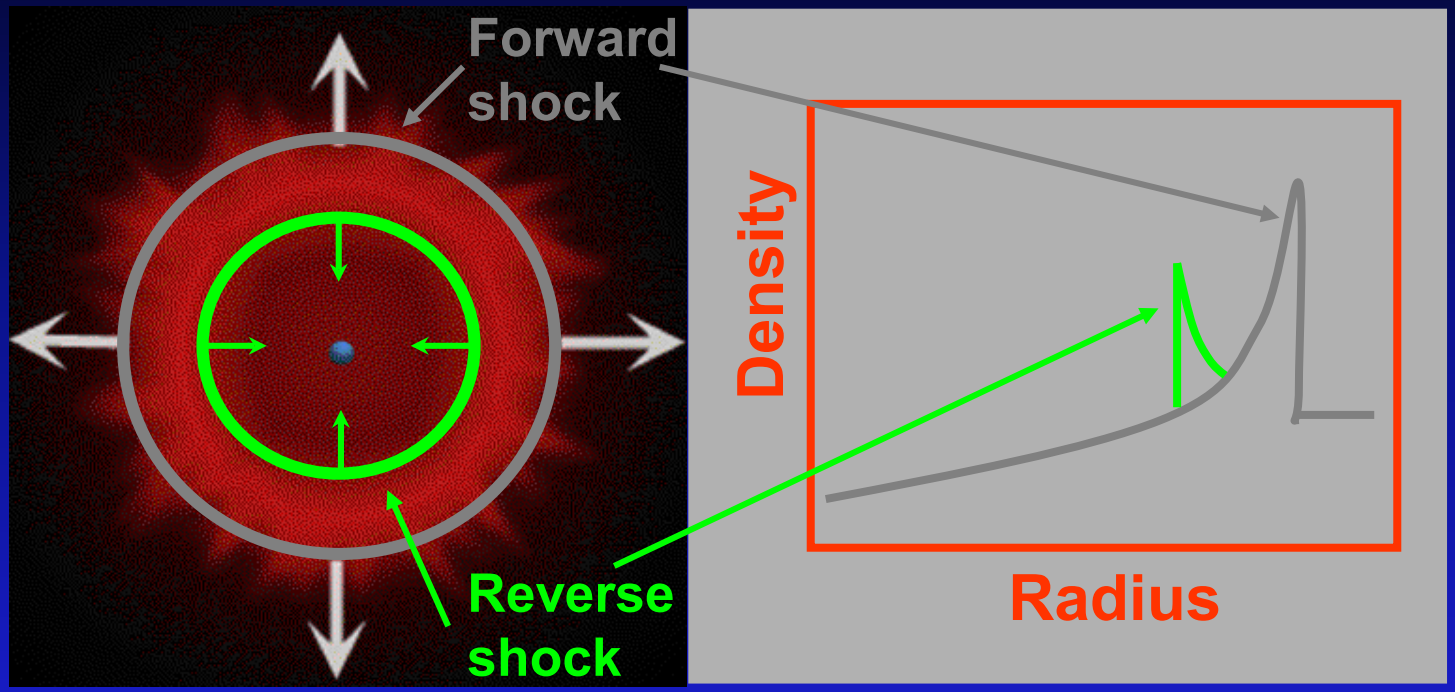

- Forward Shock: into the CSM/ISM (fast)
- Reverse Shock: into the Ejecta (slow)

自由相：Self-similar models

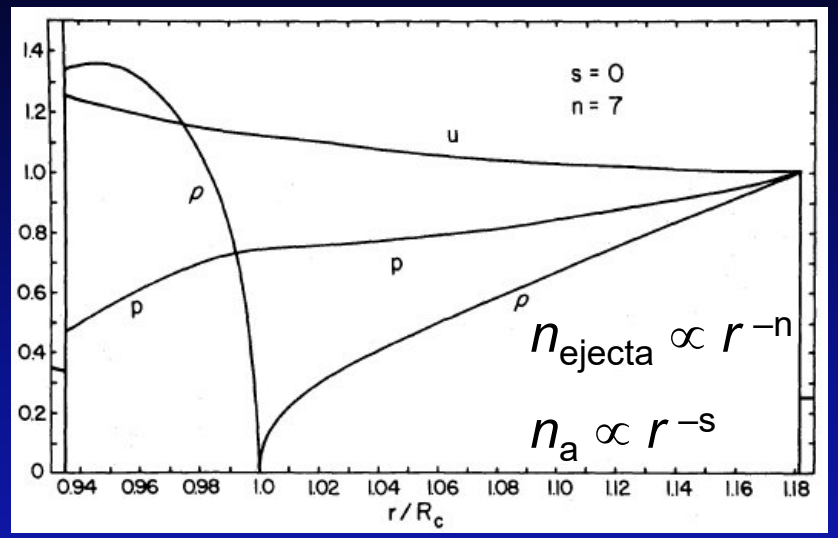

(Chevalier 1982)

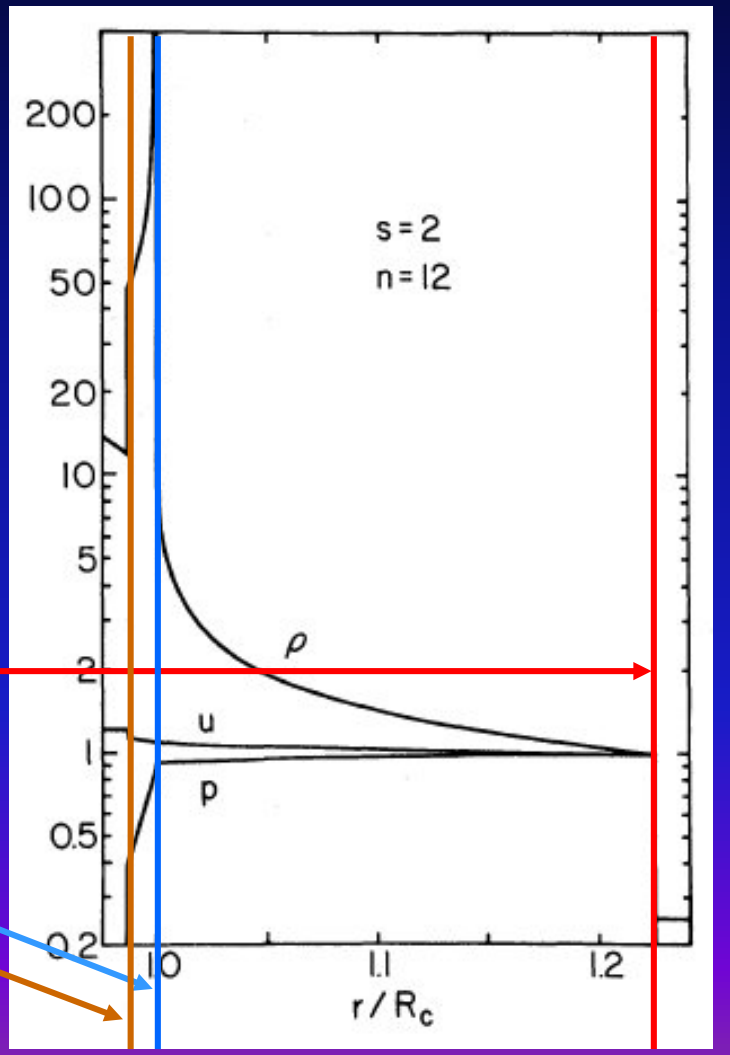

- Radial profiles
  - Ambient medium
  - Forward shock
  - Contact discontinuity
  - Reverse shock
  - Expanding ejecta

End of the free-exp. phase

Swept-up mass ~ Ejecta mass

- Reverse shock has reached the core region of the ejecta (constant density)/the center
- ~2/3 E_k has been thermalized

See Truelove & McKee (1999) for a semi-analytic treatment of this phase

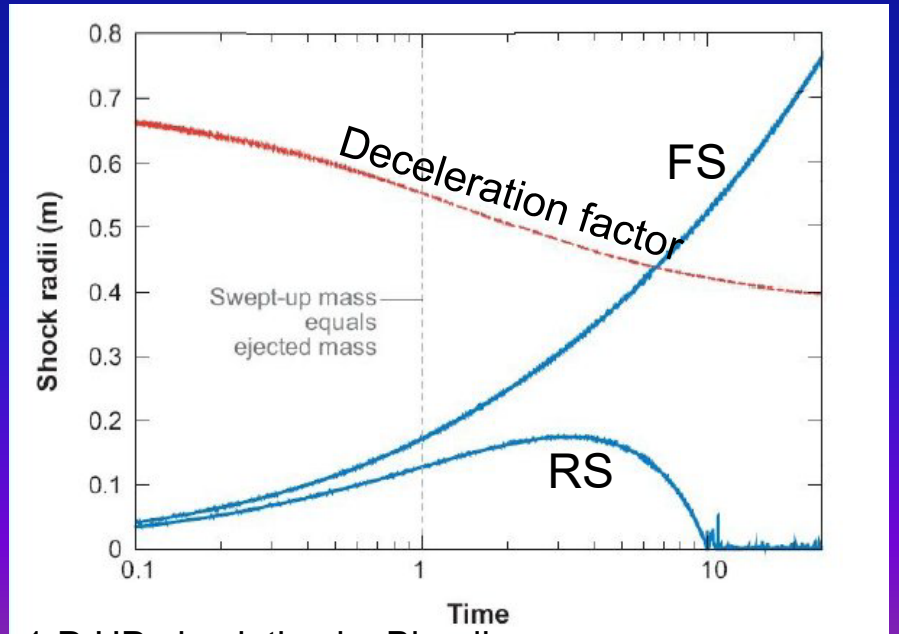

1-D HD simulation by Blondin

绝热相：The Sedov profiles

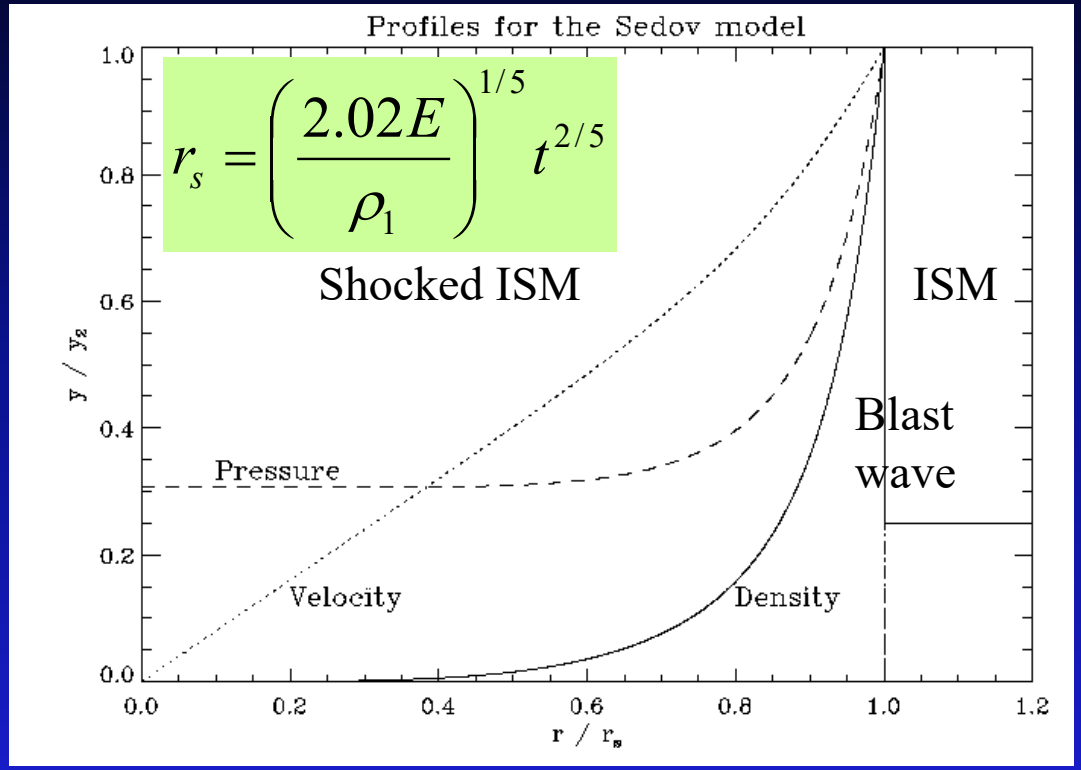

- Most of the mass is confined in a "thin" shell
- Kinetic energy is also confined in that shell
- Most of the internal energy in the "cavity"

Radiative phase

Shock wave gets so slow that
postshock gas is at a temperature

$$T_S < 6\times10^5 \text{ K}$$

and the shock wave is radiative.

$$R_S = (147 \times \epsilon E_{SNR} R_T^2 / 4\pi\rho_0)^{1/7} t^{2/7}$$

ϵ =0.24, R_T: radius at phase transition

(Blinnikov et al. 1982)

Radiative shocks

早先受到震激的(shocked)物质已冷却

$$N_{\rm rad} \cong 10^{17.5} {V_{s7}}^4 \ {\rm cm}^{-2} \ (60 < V_s < 150 \ {\rm km\ s}^{-1})$$

$$t_{\rm cool} = N_{\rm rad} / n_0 V_s \approx 10^3 {V_{s7}}^3 / n_0 \ {\rm yr}$$

$$F = \frac{1}{4} n_0 \mu \, m_{\rm H} \, V_s^3 = 5.8 \times 10^{-4} n_0 {V_{s7}}^3 \ {\rm ergs\ cm}^{-2}\ {\rm s}^{-1}$$

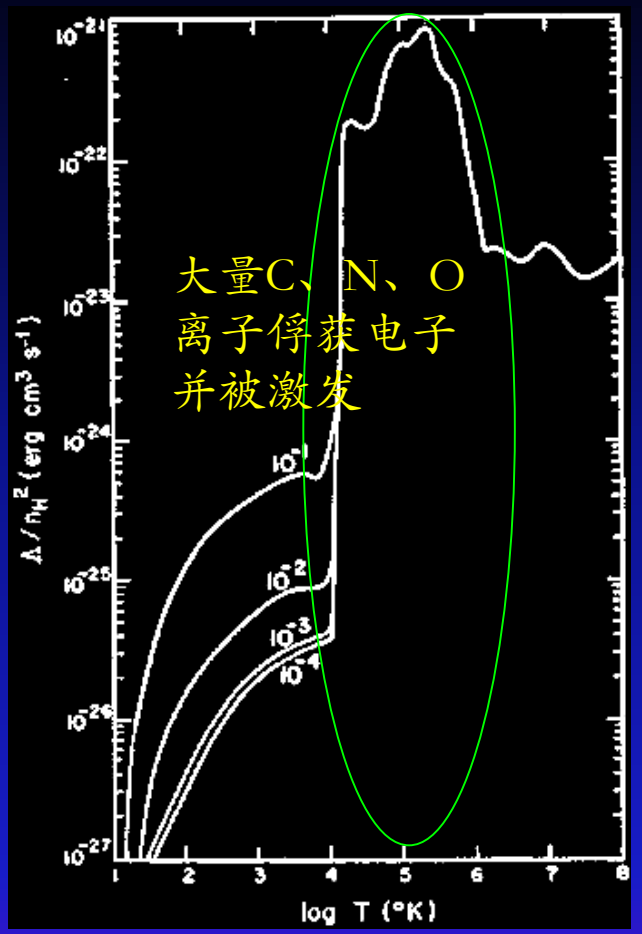

- 辐射性前导 (Radiative precursor):
  UV光子电离 （V_s > 110 km/s可完全电离H、He）
  分子气体： 光致离解 （$H_2 \rightarrow H+H$）进而电离

- 跃变条件：

$T_1 = T_2$ （等温，相当于 γ=1）

$$\frac{\rho_2}{\rho_1} = \frac{4}{\frac{2}{M^2} + \frac{1}{{M_A}^2} + \left[\left(\frac{2}{M^2} + \frac{1}{{M_A}^2} \right)^2 + \frac{8}{{M_A}^2} \right]^{1/2}}$$

$\sqrt{} \rightarrow \sqrt{2} M_A \quad (1 << M_A << M^2)$

$\sqrt{} \rightarrow M^2 \quad (1 \le M^2 << M_A)$

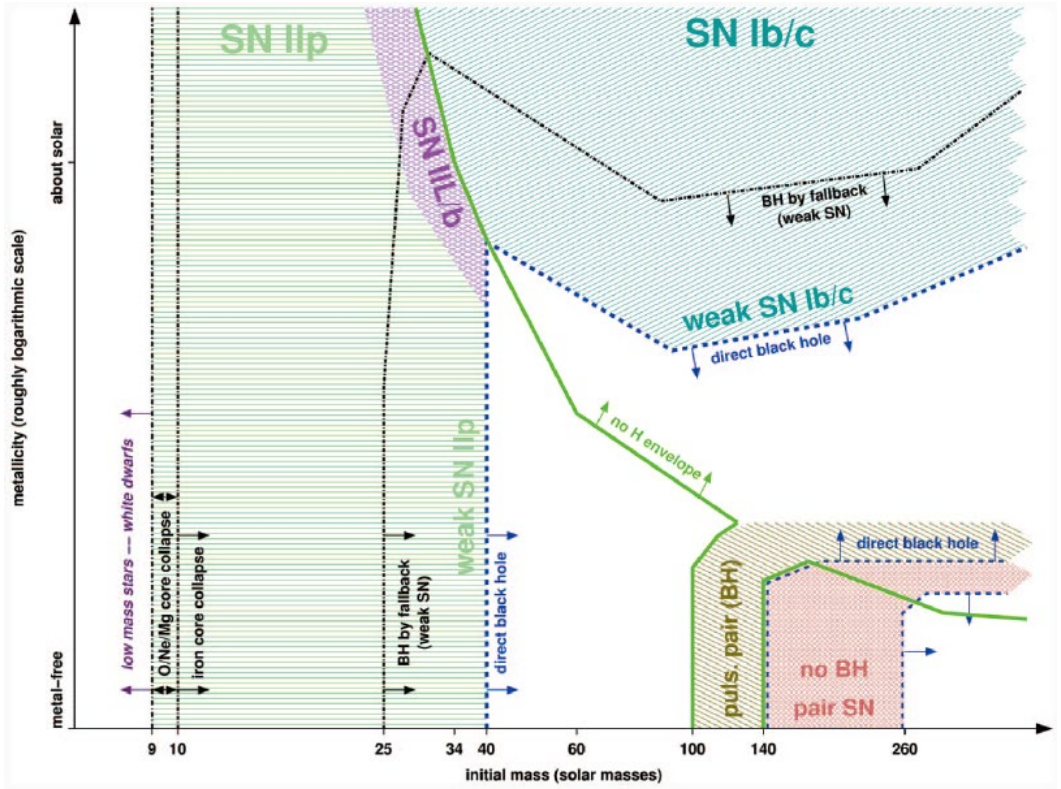
SN IIp
SN Ib/c
SN IIL/b
BH by fallback
(weak SN)
weak SN Ib/c
direct black hole
no H envelope
weak SN IIp
direct black hole
puls. pair (BH)
direct black hole
no BH
pair SN
metallicity (roughly logarithmic scale)
about solar
metal–free
low mass stars → white dwarfs
O/Ne/Mg core collapse
iron core collapse
BH by fallback
(weak SN)
direct black hole
9 10 25 34 40 60 100 140 260
initial mass (solar masses)

Heger+2003

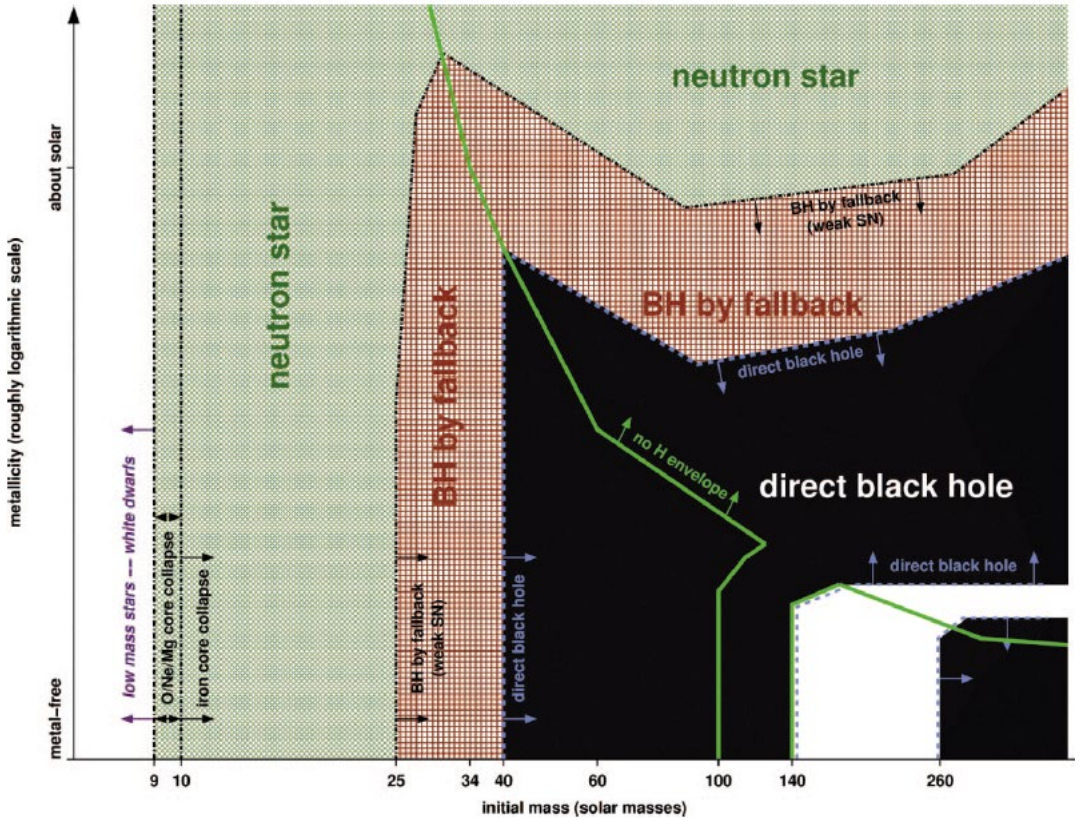
neutron star
neutron star
BH by fallback
BH by fallback
(weak SN)
BH by fallback
direct black hole
no H envelope
direct black hole
direct black hole
metallicity (roughly logarithmic scale)
about solar
metal–free
low mass stars → white dwarfs
O/Ne/Mg core collapse
iron core collapse
BH by fallback
(weak SN)
direct black hole
9 10 25 34 40 60 100 140 260
initial mass (solar masses)

SNR-NS associations

(Credit: Fu, Lei)

	PSRJ	P	P_dot	ASSOC	Age	B_surf	SNR age(yr)
2	J0007+7303	0.315873192	3.60550E-13	GRS:1FGL_J0007.0+7303,XRS:RX_J	1.39e+04	1.08e+13	5k-15k
3	J0205+6449	0.065715928	1.93754256E-13	SNR:3C58,GRS:1FGL_0205.6+6449[	5.37e+03	3.61e+12	830-7k
4	J0525-6607	8.047	6.5E-11	XRS:SGR_0526-66,SNR:N49(?)[ekl+	1.96e+03	7.32e+14	5k-10k
5	J0534+2200	0.033084716	4.22765E-13	SNR:Crab_PWN[ccl+69],GRS:1FGL_	1.24e+03	3.78e+12	
6	J0537-6910	0.016122222	5.1784338E-14	EXGAL:LMC,SNR:N157B	4.93e+03	9.25e+11	<5k
7	J0538+2817	0.143158259	3.6694515E-15	SNR:S147[acj+96]	6.18e+05	7.33e+11	20k-100k
8	J0540-6919	0.050498818	4.78924621E-13	EXGAL:LMC,SNR:0540-693	1.67e+03	4.98e+12	760-1660
9	J0633+0632	0.297395191	7.9592E-14	GRS:1FGL_J0633.7+0632,XRS:Swift_	5.92e+04	4.92e+12	*
10	J0659+1414	0.384891195	5.500309E-14	SNR:Monogem_Ring[tbb+03],GRS:1F	1.11e+05	4.66e+12	86k
11	J0821-4300	0.112799437	1.2E-15	SNR:PUPPIS_A,XRS:RX_J0822-4300	1.49e+06	3.72e+11	3.7k
12	J0835-4510	0.089328385	1.25008E-13	SNR:Vela,GRS:1FGL_J0835.3-4510[	1.13e+04	3.38e+12	11k-12.3k
13	J0855-4644	0.064686131	7.26269E-15	SNR:RX_J0852.0-4622(?)[rm05]	1.41e+05	6.94e+11	1.7k-4.3k
14	J1016-5857	0.107386458	8.08342E-14	SNR:G284.3-1.8(?)	2.1e+04	2.98e+12	10k
15	J1119-6127	0.407962984	4.0202200E-12	SNR:G292.2-0.5[cgk+01]	1.61e+03	4.1e+13	3k
16	J1124-5916	0.135476854	7.52566E-13	SNR:G292.0+1.8,GRS:1FGL_J1124.(	2.03e+04	1.02e+13	2.7k-3.7k
17	J1210-5226	0.424130749	6.6E-17	SNR:G296.5+10.0;XRS:1E_1207.4-5	1.02e+08	1.69e+11	10k
18	J1341-6220	0.193339746	2.53107E-13	SNR:G308.8-0.1[cks+92]	1.21e+04	7.08e+12	32.5k
19	J1437-5959	0.061696123	8.5870E-15	SNR:G315.9-0.0	1.14e+05	7.37e+11	22k
20	J1513-5908	0.150657551	1.53652913E-12	SNR:G320.4-1.2(MSH 15-52),GRS:1F	1.55e+03	1.54e+13	6k-20k
21	J1550-5418	2.06983302	2.318E-11	XRS:1E_1547.0-5408[gg07],SNR:G32	1.41e+03	2.22e+14	*
22	J1632-4818	0.813452834	6.50425E-13	SNR:G336.1-0.2(?)[mbc+02]	1.98e+04	2.33e+13	*
23	J1635-4735	2.594578	*	XRS:SGR_1627-41,SNR:G337.0-0.1('	*	*	*
24	J1646-4346	0.231603329	1.12753E-13	SNR:G341.2+0.9(?)[fgw94]	3.25e+04	5.17e+12	*
25	J1709-4429	0.102459246	9.298454E-14	SNR:G343.1-2.3(?)[mop93],GRS:HES	1.75e+04	3.12e+12	5k
26	J1726-3530	1.110132444	1.216751E-12	SNR:G352.2-0.1(?)[mbc+02]	1.45e+04	3.72e+13	*
27	J1747-2809	0.052152855	1.5557E-13	XRS:CXOU_J174722.8-280915,SNR:(	5.31e+03	2.88e+12	1k-7k
28	J1801-2451	0.124924207	1.279057E-13	SNR:G5.4-1.2[fk91],XRS:PWN[kggl0	1.55e+04	4.04e+12	14k
29	J1801-2304	0.41582709	1.1293023E-13	SNR:W28(?)[fkv93]	5.83e+04	6.93e+12	35k-150k(42
30	J1803-2137	0.13366692	1.34359375E-13	SNR:G8.7-0.1(?)[kw90],GRS:J1804-2	1.58e+04	4.29e+12	15k-39k
31	J1808-2024	7.55592	5.49E-10	SNR:G10.0-0.3(W31),SGR_1806-20	218	2.06e+15	3k-10k
32	J1809-2332	0.146788548	3.44207E-14	GRS:1FGL_J1809.8-2332,XRS:CXOU	6.76e+04	2.27e+12	10k-100k
33	J1811-1925	0.064667	4.40E-14	SNR:G11.2-0.3	2.33e+04	1.71e+12	1.6k(AD386?
34	J1813-1749	0.044699298	1.5E-13	SNR:12.8-0.0,GRS:HESS_J1813-178	4.6e+03	2.65e+12	285-2.5k
35	J1833-1034	0.061865672	2.02025e-13	SNR:G21.5-0.9[gmga05],SN:BC48[wl	4.85e+03	3.58e+12	200-1k
36	J1841-0456	11.7789433	4.470E-11	SNR:Kes73,XRS:1E_1841-045	4.18e+03	7.34e+14	500-2k
37	J1845-0256	6.97127	*	SNR:G29.6+0.1,AX_J1845.0-0300	########	*	1.4k-8k
38	J1846-0258	0.325684249	7.08330E-12	SNR:Kes75,XRS:PWN[hcg03]	728	4.86e+13	0.9k-4.3k
39	J1850-0006	2.191497968	4.32E-15	SNR:G32.45+0.1(?)	8.04e+06	3.11e+12	*
40	J1852+0040	0.104912611	8.68E-18	SNR:Kes79,XRS:CXOU_J185238.6+0	1.92e+08	3.05e+10	3k-7.8k
41	J1856+0113	0.26743961	2.083598E-13	SNR:W44,XRS:PWN[pks02]	2.03e+04	7.55e+12	7k,5k
42	J1907+0602	0.106632746	8.68208E-14	GRS:1FGL_J1907.9+0602,SNR:G40.	1.95e+04	3.08e+12	20k-40k
43	J1907+0919	5.1689178	7.783E-11	SNR:G42.8+0.6(?),SGR_1900+14	1.05e+03	6.42e+14	15.5k
44	J1930+1852	0.136855047	7.5057E-13	SNR:G54.1+0.3,XRS	2.89e+03	1.03e+13	2.5k-3.3k
45	J1952+3252	0.039531193	5.844803E-15	SNR:CTB80,GRS:1FGL_J1952.9+32	1.07e+05	4.86e+11	77k
46	J1957+2831	0.307682865	3.10989E-15	SNR:G65.1+0.6[tl06]	1.57e+06	9.9e+11	44k-140k
47	J2021+4026	0.265317661	5.4682E-14	GRS:1FGL_J2021.5+4026,SNR:G78.	7.69e+04	3.85e+12	4k-7k
48	J2022+3842	0.024287756	4.3192E-14	XRS:CXOU_J202221.68+384214.8,SN	8.91e+03	1.04e+12	5k
49	J2229+6114	0.051623574	7.827E-14	SNR:G106.6+2.9,GRS:1FGL_J2229.(	1.05e+04	2.03e+12	10k
50	J2301+5852	6.978948446	4.8430E-13	SNR:CTB109,XRS:1E_2259.1+586	2.28e+05	5.88e+13	6.7k-21k
51	J2337+6151	0.495369868	1.934498E-13	SNR:G114.3+0.3[frs93]	4.06e+04	9.91e+12	10k-100k

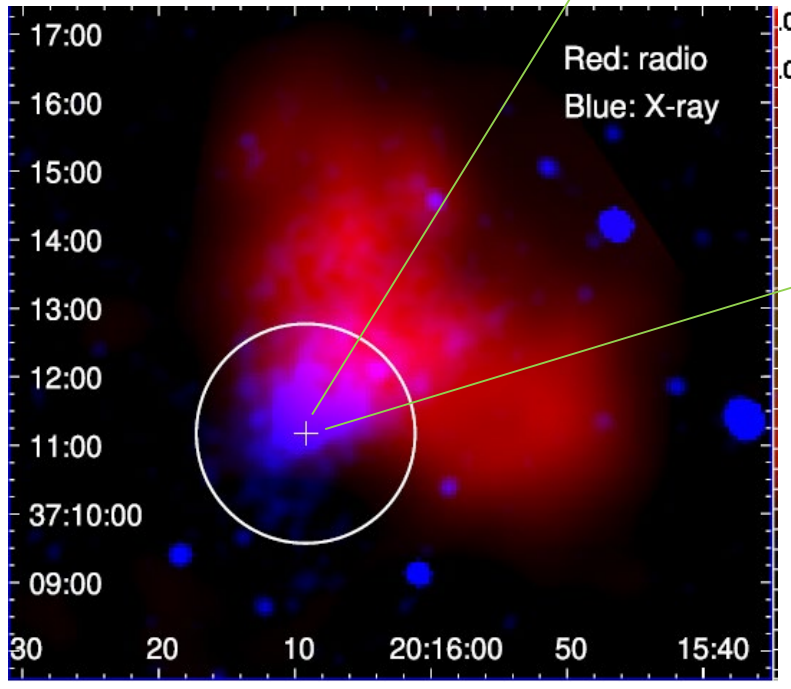

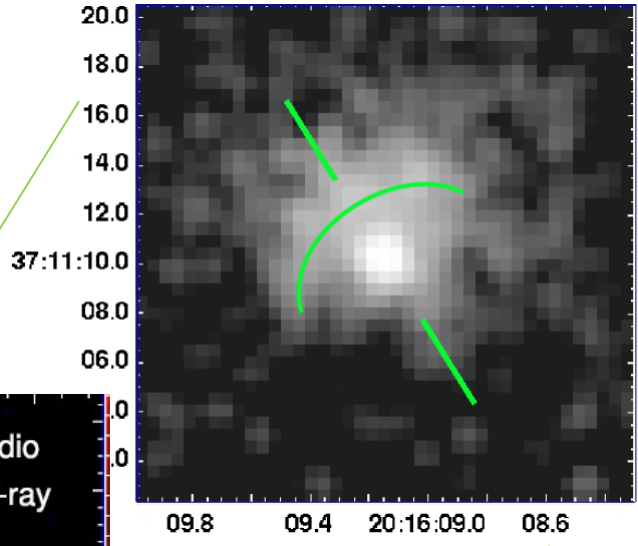

(Matheson+13)

Latest discovered association: the **51ms** pulsar in CTB87, discovered with FAST

(Liu, Zhong, Chen+24)

Pulsar wind nebula (PWN)

Magnetized particle wind: e+, e-

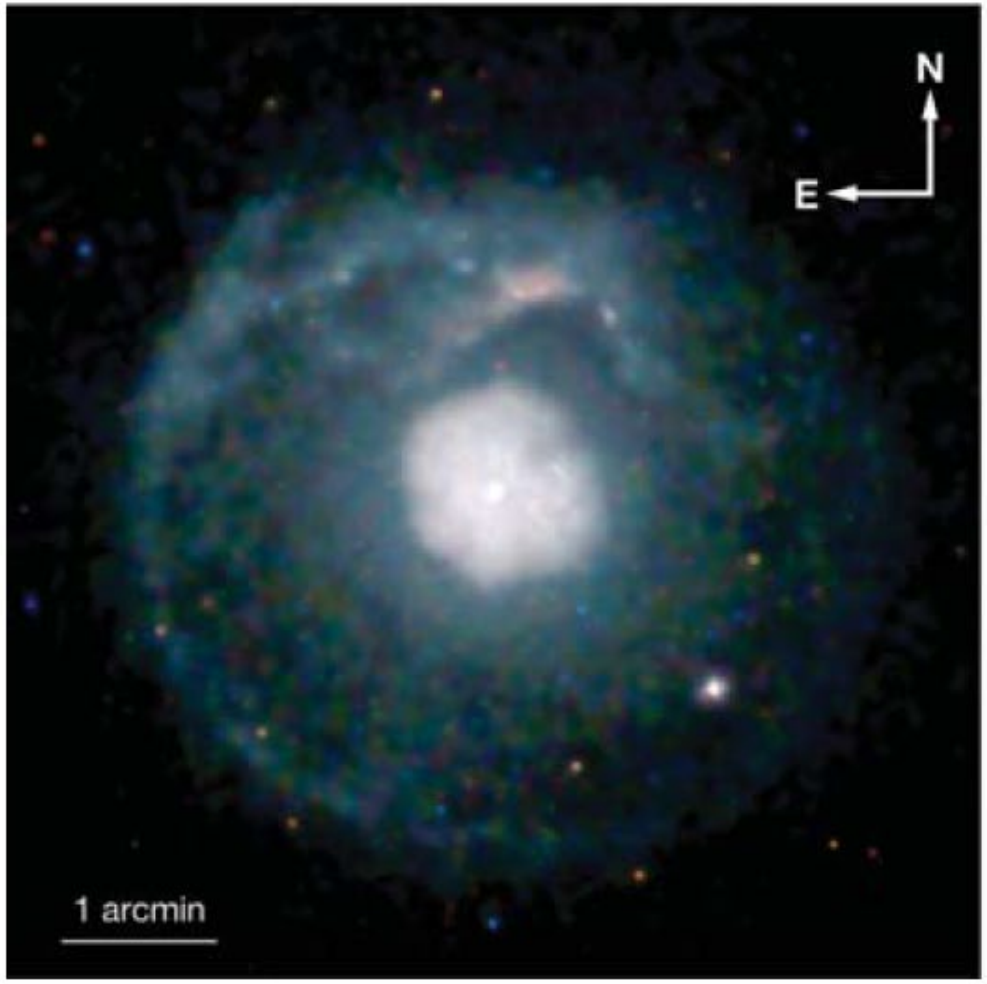

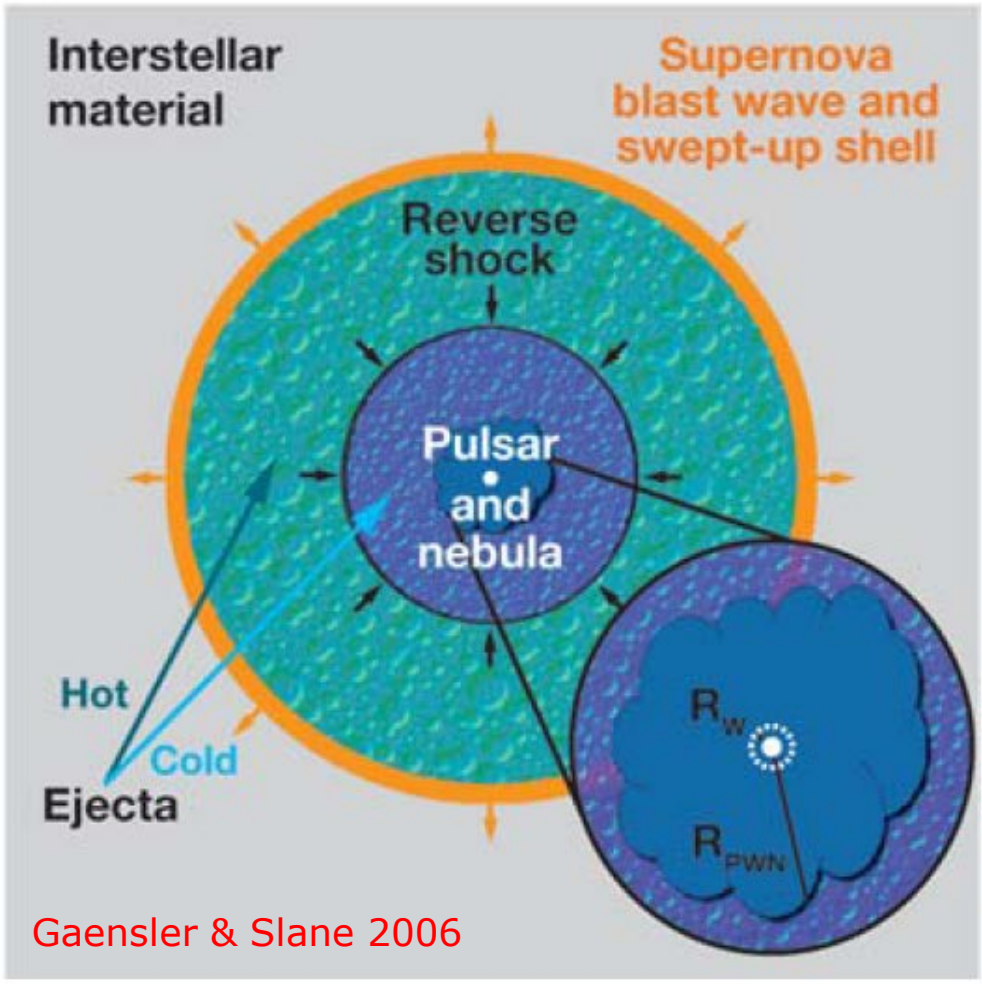

Termination shock: $R_W = [\dot{E}/(4\pi\omega c\, P_{PWN})]^{1/2}$

The "Crab"

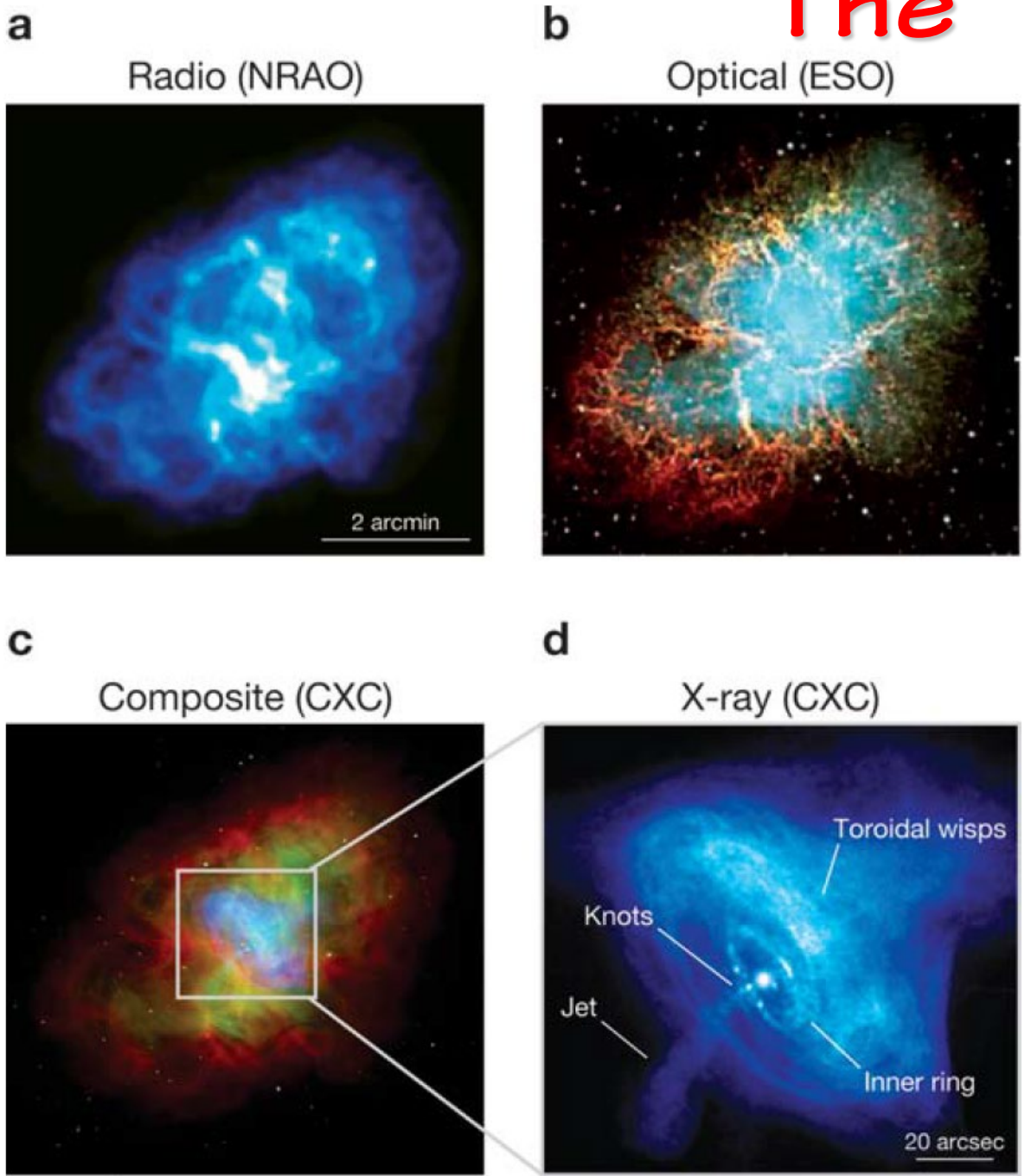

Magnetization parameter:

$$\sigma \equiv \frac{F_{E\times B}}{F_{\text{particle}}} = \frac{B^2}{4\pi\rho\gamma c^2}$$

□ 1

Particle dominated wind, with $\gamma \sim 10^6$

Kennel & Coroniti 1984

Torus+jets structure

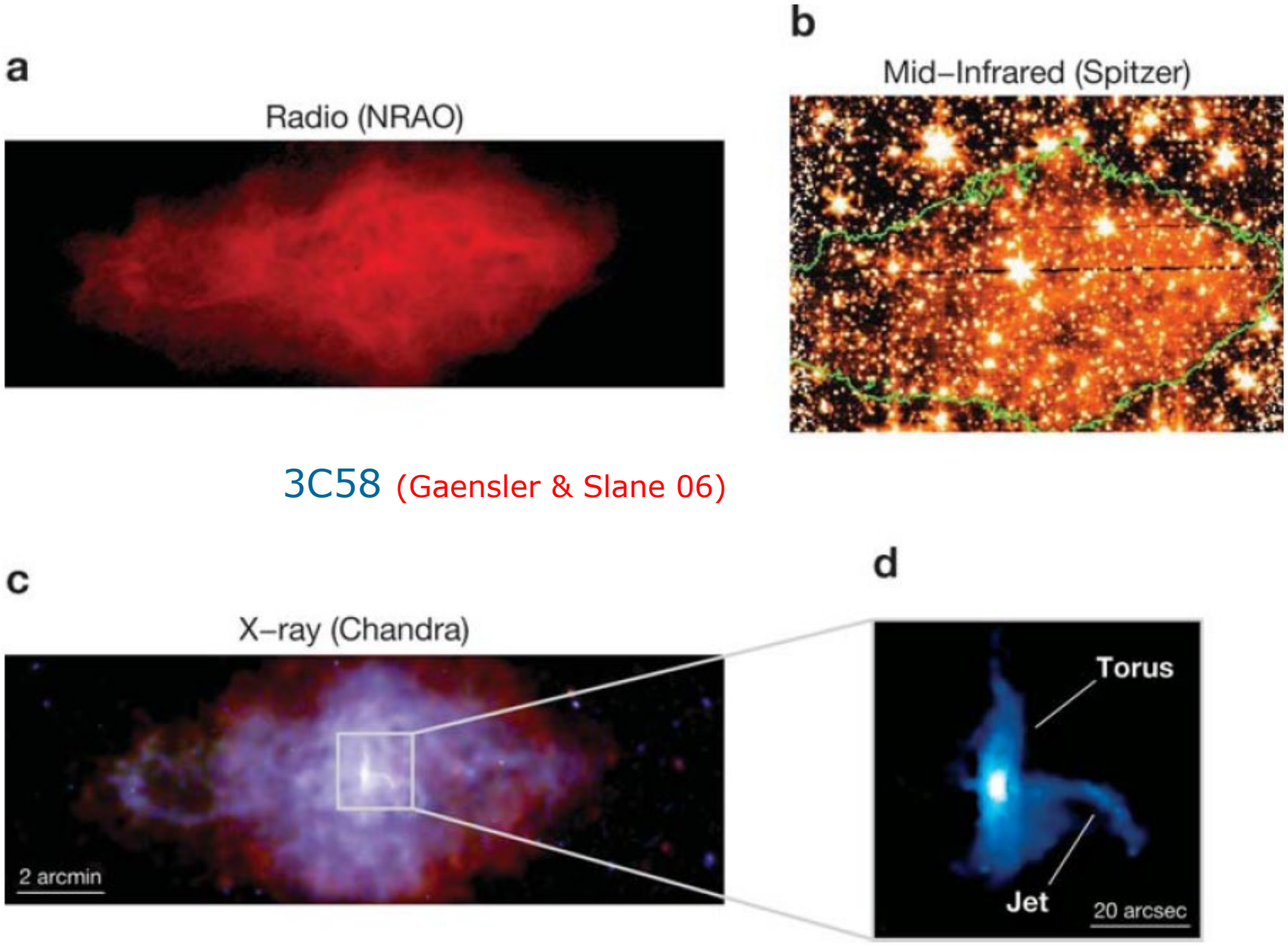

3C58 (Gaensler & Slane 06)

G54.1+0.3

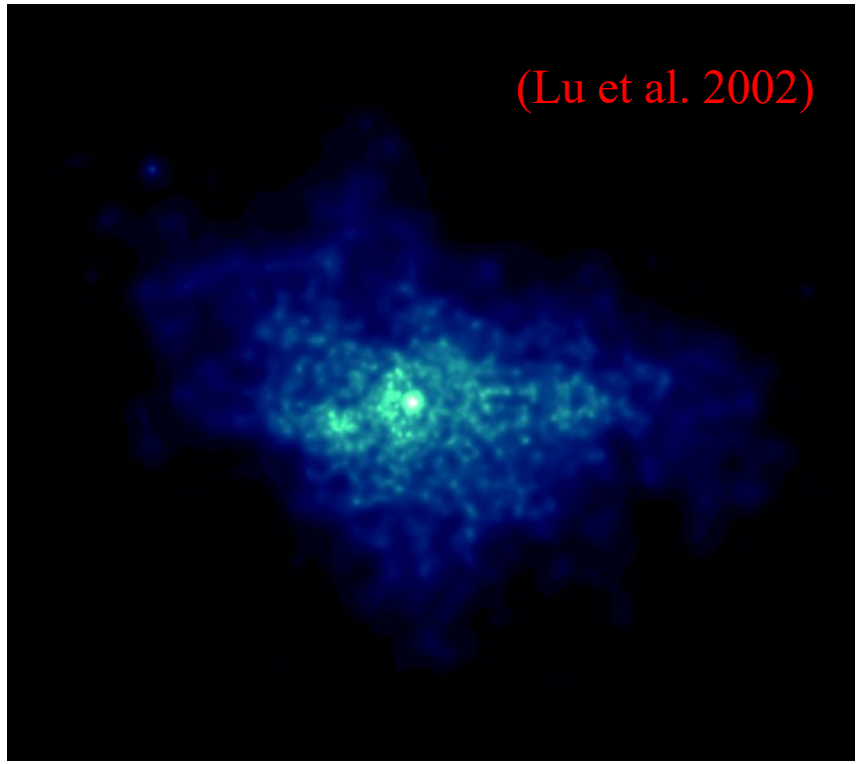

CTB 87

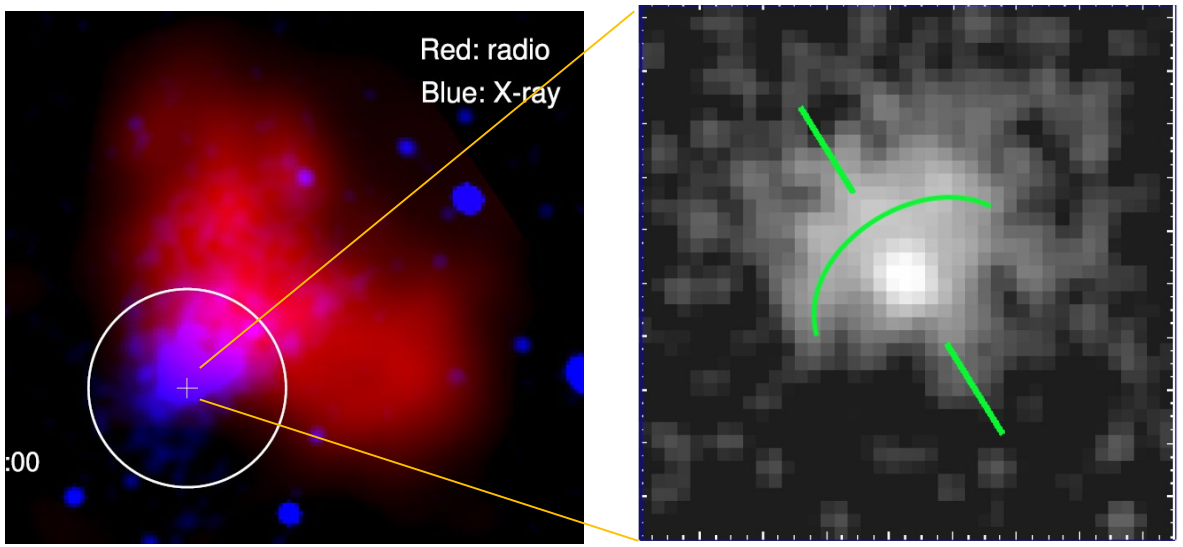

(Liu, Zhong, Chen+ 2024)

(Matheson+ 2013)

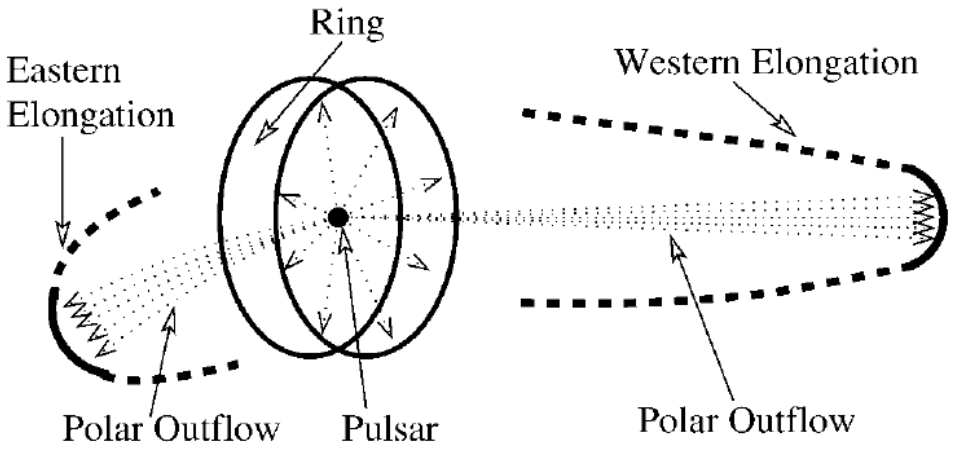

The wind of the central pulsar can be divided into two components: equatorial flow and polar flow.

Spectral indices

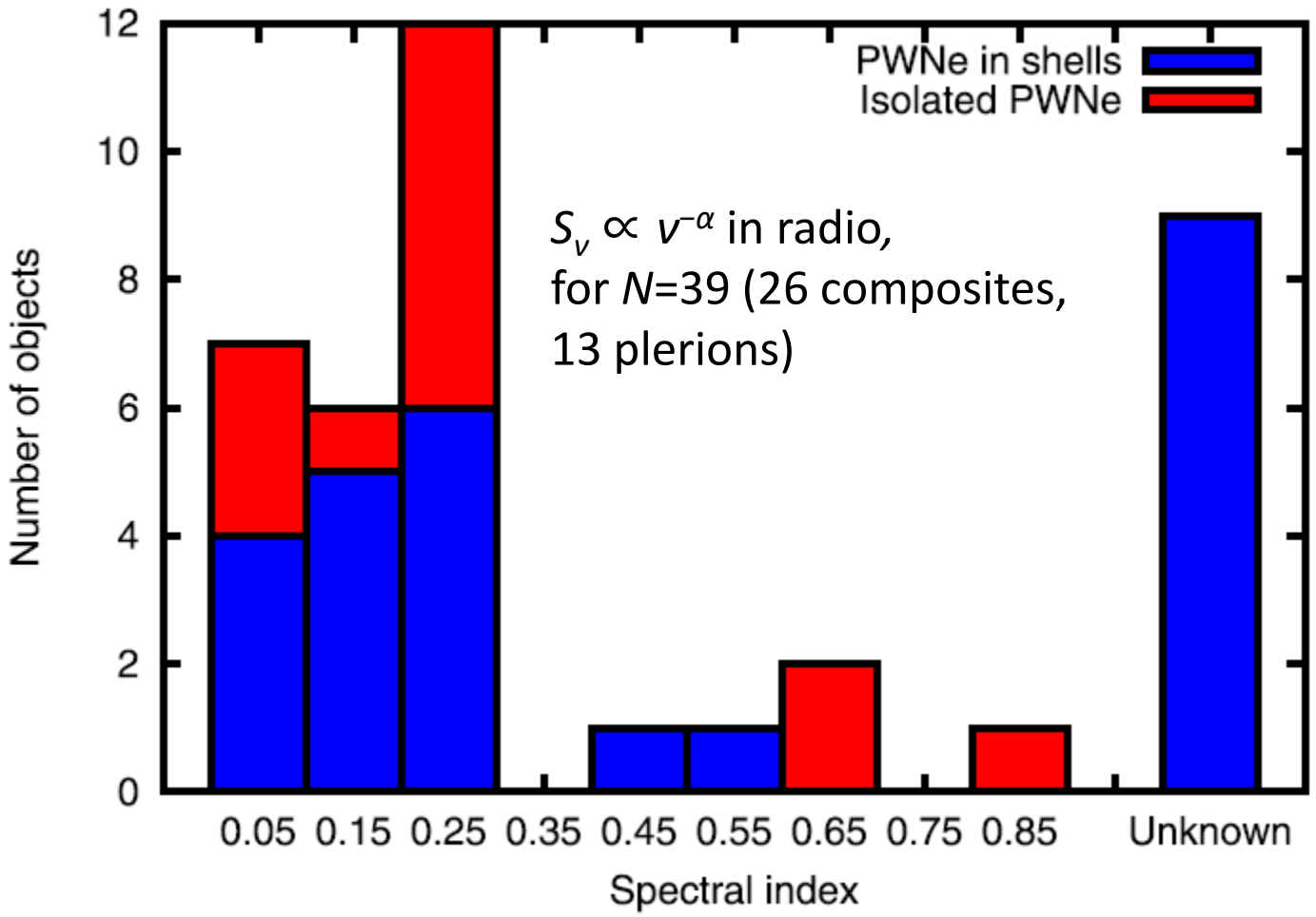

Seward-Wang Relation

汪珍如教授 1937-2017

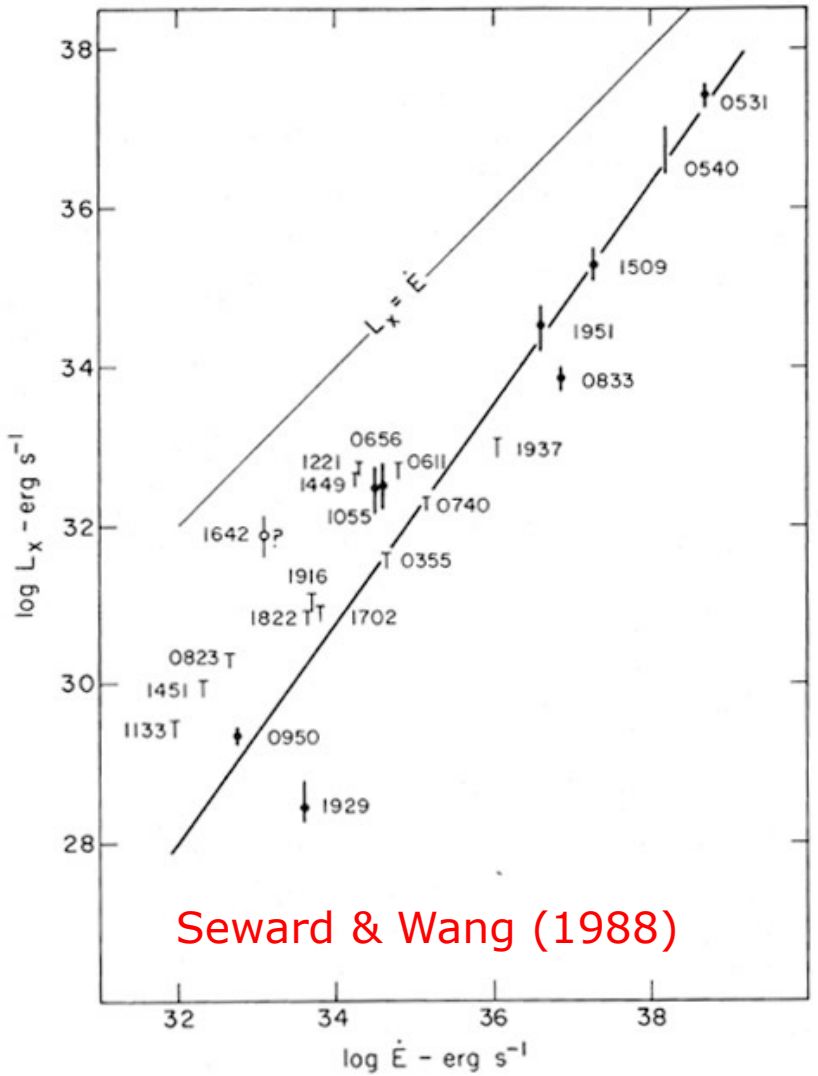

Seward & Wang (1988)

…… she pioneered X-ray astronomy in China.
- Richard McCray (1937-2021)

Relations between the X-ray luminosity and spin-down power (with a sample of 24 PWNe)

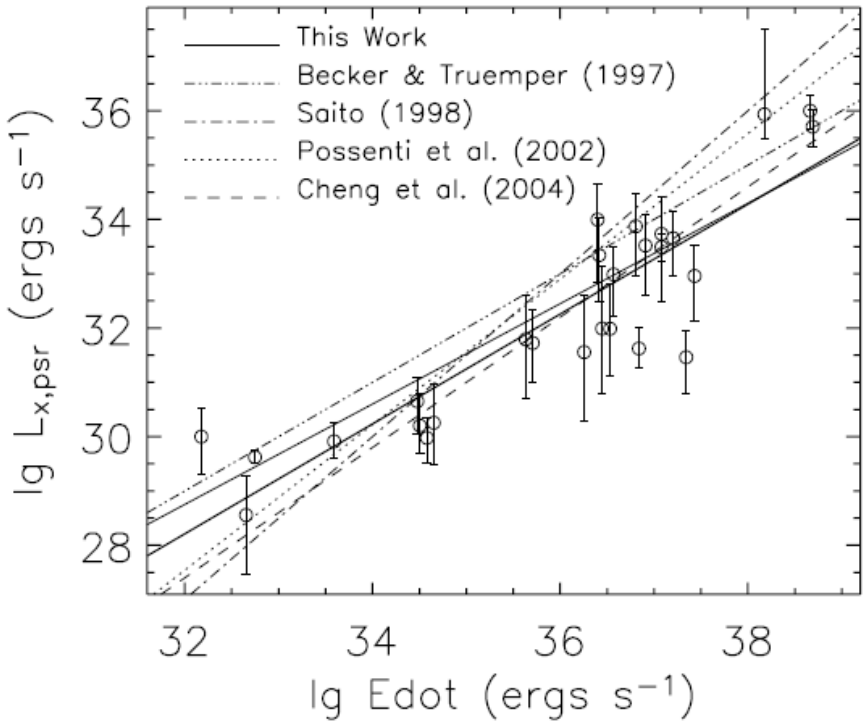

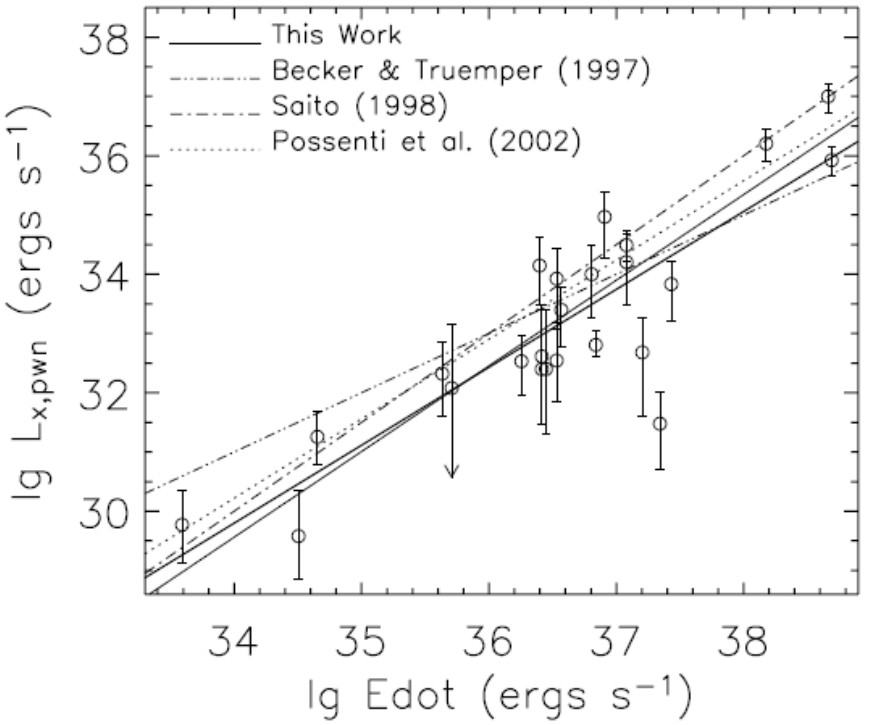

$$L^{*}_{\mathrm{X,\,psr}} = 10^{-4.2\pm3.7}\dot{E}^{1.0\pm0.1}$$

$$L^{*}_{\mathrm{X,\,pwn}} = 10^{-14.9\pm6.0}\dot{E}^{1.3\pm0.2}$$

The more energetic pulsars intend to release a bigger fraction of their spin-down power in their PWNe.

Li, Lu & Li 2008, ApJ 682, 1166

Synchrotron loss

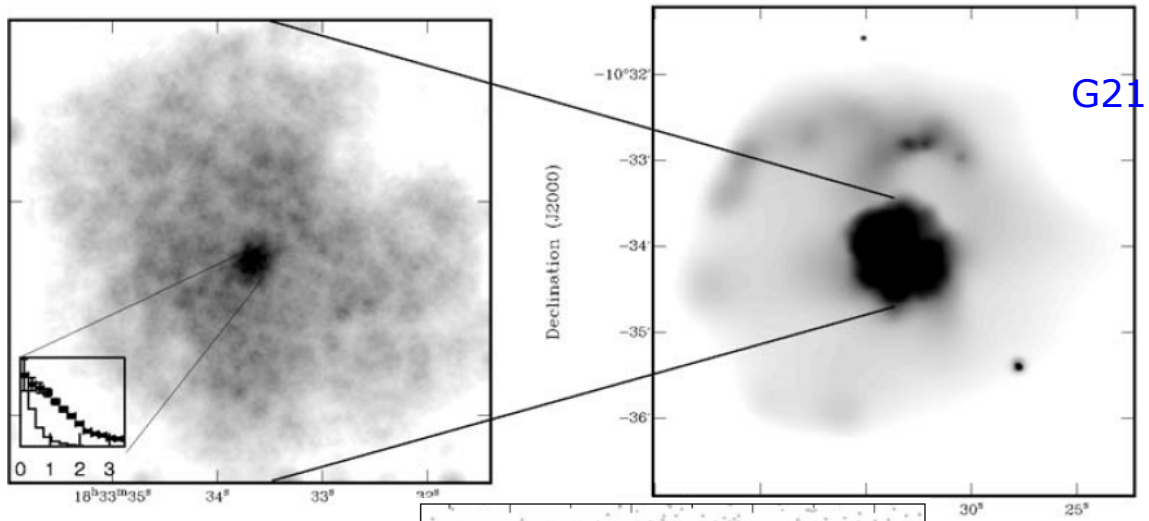

G21.5-0.9

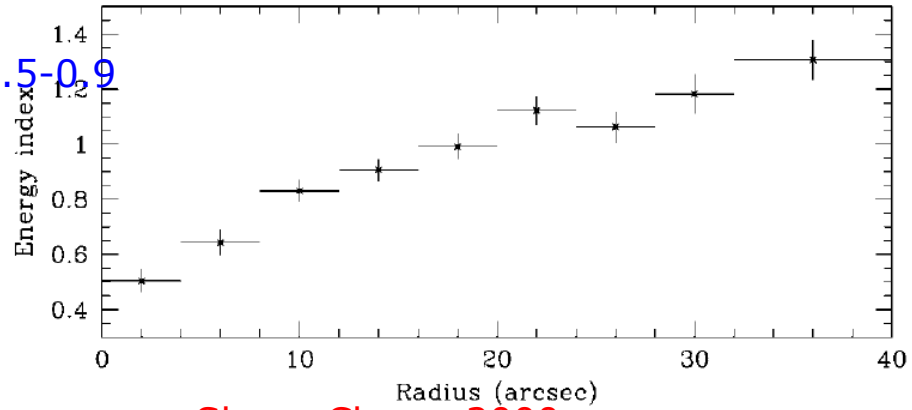

Slane, Chen+ 2000, Chandra

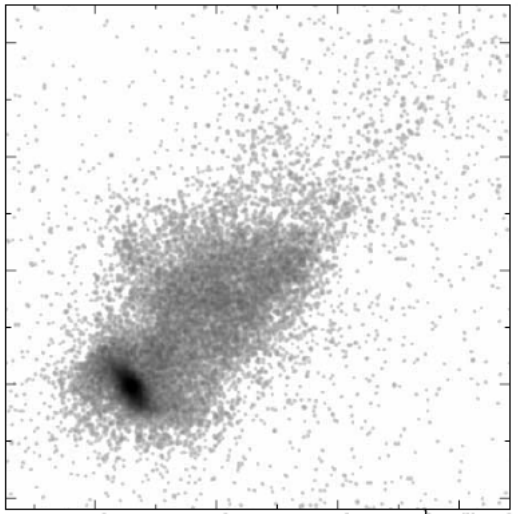

$$dE/dt \propto E^2 B^2$$

$$\Rightarrow \quad \bar{\Gamma} = \frac{p+1}{2} + \frac{p-1}{2} \frac{\left(\sqrt{\varepsilon_m/\varepsilon_l} - 1\right)^{p-2} - \left(\sqrt{\varepsilon_m/\min(\varepsilon_u, \varepsilon_m)} - 1\right)^{p-2}}{\left(\sqrt{\varepsilon_m/\varepsilon_l} - 1\right)^{p-1} - \left(\sqrt{\varepsilon_m/\min(\varepsilon_u, \varepsilon_m)} - 1\right)^{p-1}}$$

N157B

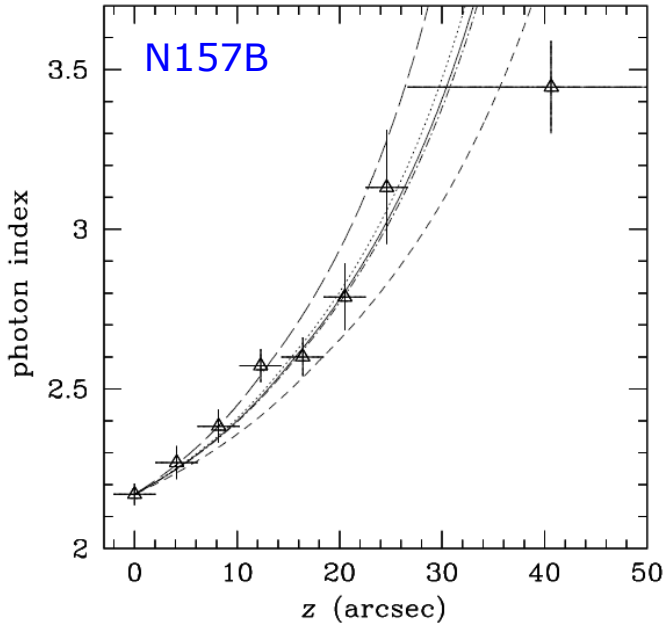

Chen+ 2006

Evolution of PWNe

(1) 在脉冲星减速时标τ以内（$t < \tau$）,受到终止激波震击的超高压的脉冲星风等离子体在抛射物的核区内迅速向外扩张形成小泡，表面激波依$\propto t^{6/5}$超声速加速膨胀。

(2) 泡面受到从遗迹壳层传回的反向激波碰撞（发生的典型时标为几千年），在数千年内经历若干次压缩、反弹的轮回震荡，乃至压破。

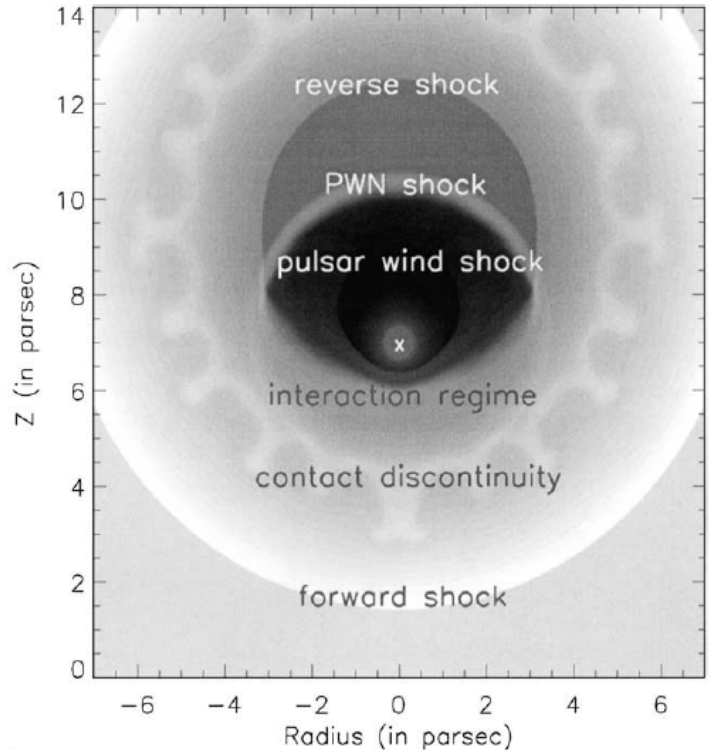

2kyr

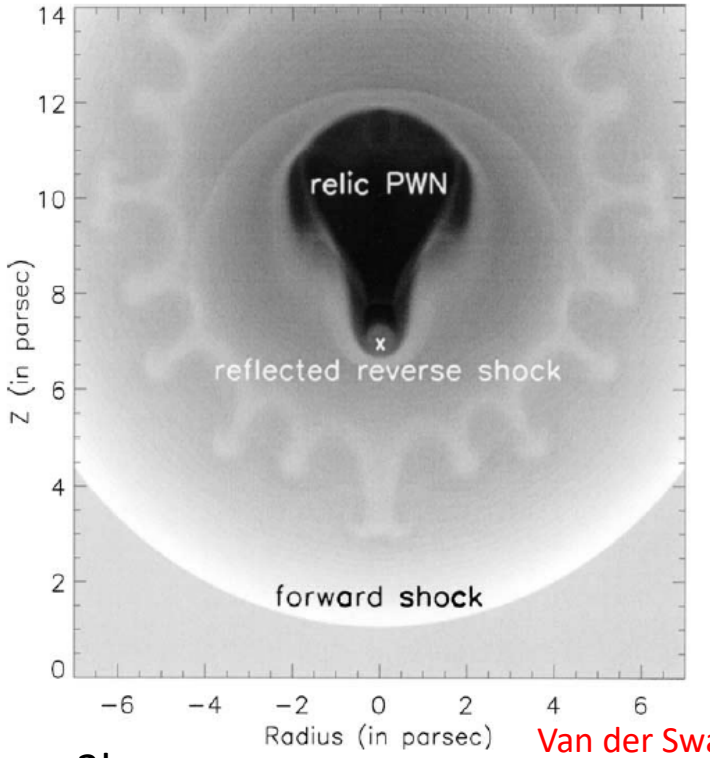

3kyr

Van der Swaluw 2004

Evolution of PWNe

(3) 脉冲星风云在处于Sedov相的遗迹内部高温气体中亚声速膨胀。若$t < \tau$，演化律为$\propto t^{11/15}$；若$t > \tau$，则按$\propto t^{0.3}$强烈减速。

(4) 由于脉冲星在超新星爆炸时获得“踢出”速度（典型值为每秒500公里上下），脉冲星穿出原先的风泡，生成新的、较小的星风云，新旧星风云各自主要呈现在X射线和射电波段。

G327.1-1.1

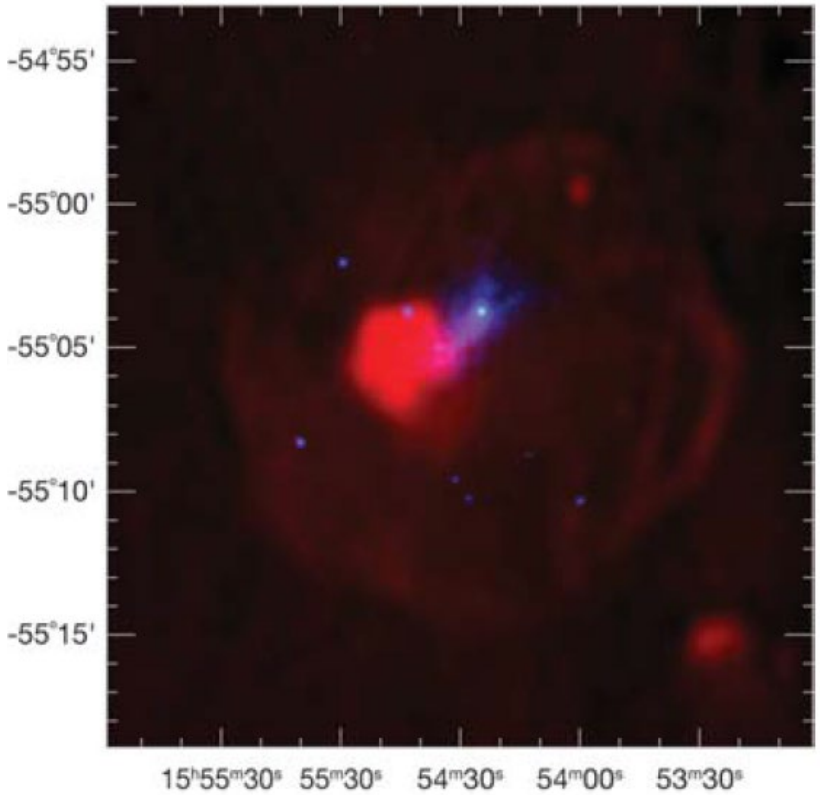

Gaensler & Slane 2006

PSR escapes from radio *relic PWN* left behind

Vela PWN

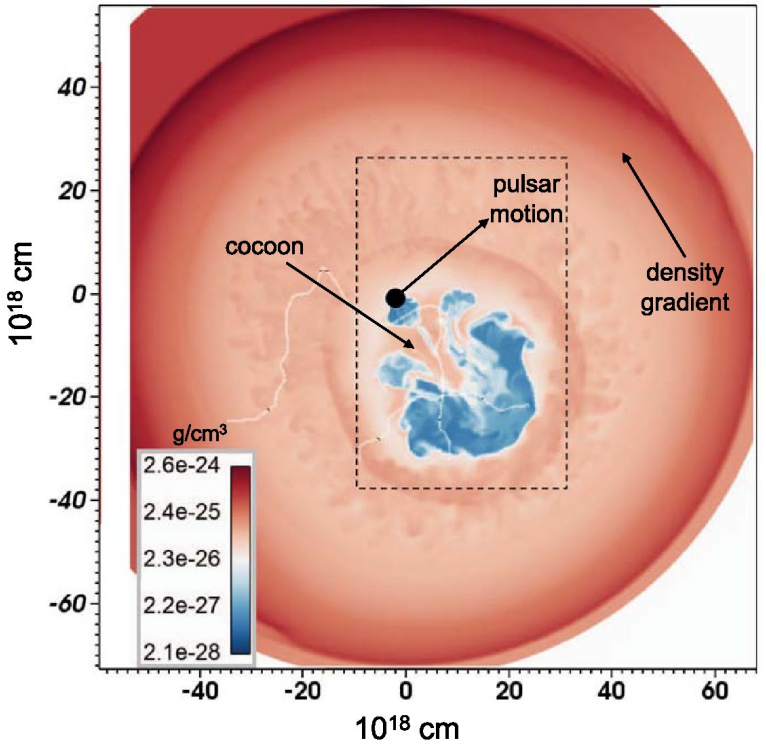

Slane+ 2018

Evolution of PWNe

(5) 随着遗迹内部气体的冷却，脉冲星的穿行成为超声速运动，星风云外表出现弓激波，呈彗星样的拖尾状，不再膨胀。

Transition to bow shock at 68% r_s

W44

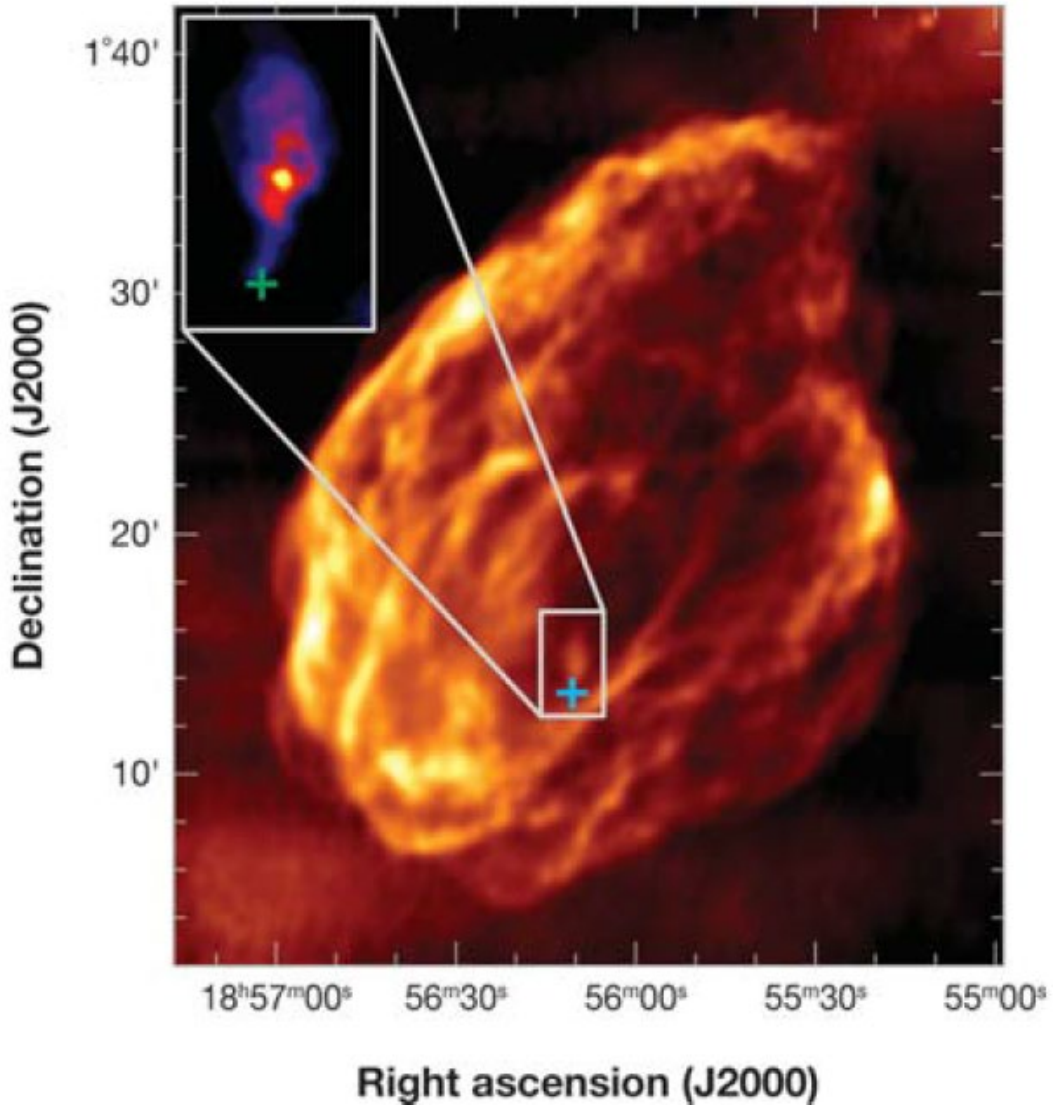

Gaensler & Slane 2006

Evolution of PWNe

PSR B1957+20 (recycled `black widow')

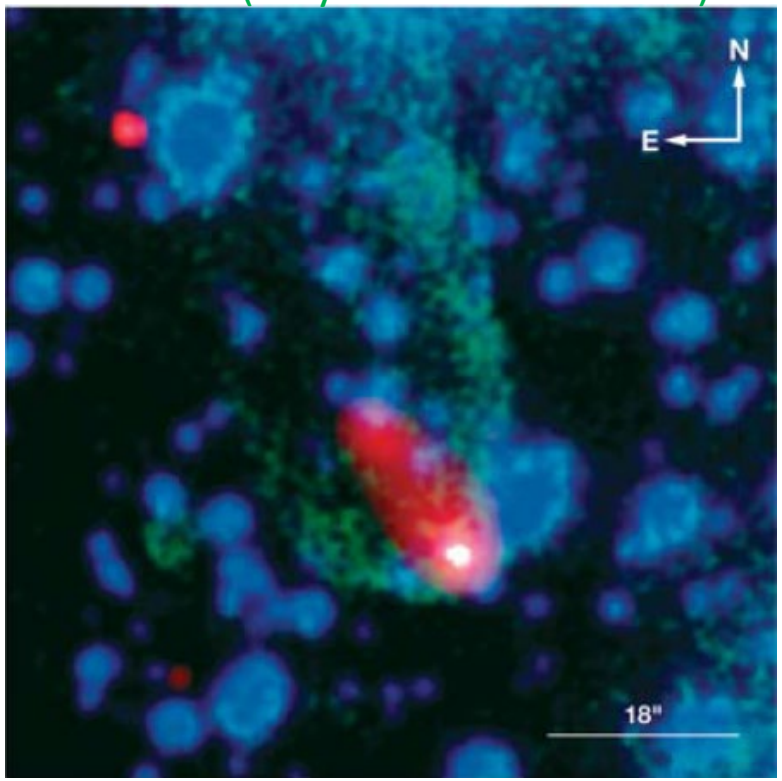

Gaensler & Slane 2006

Mouse Nebula

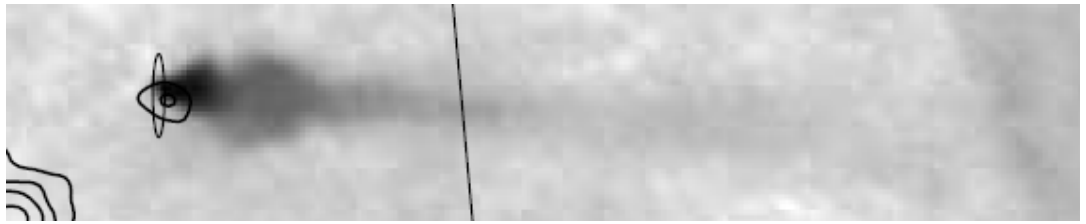

Gaensler+ 2004

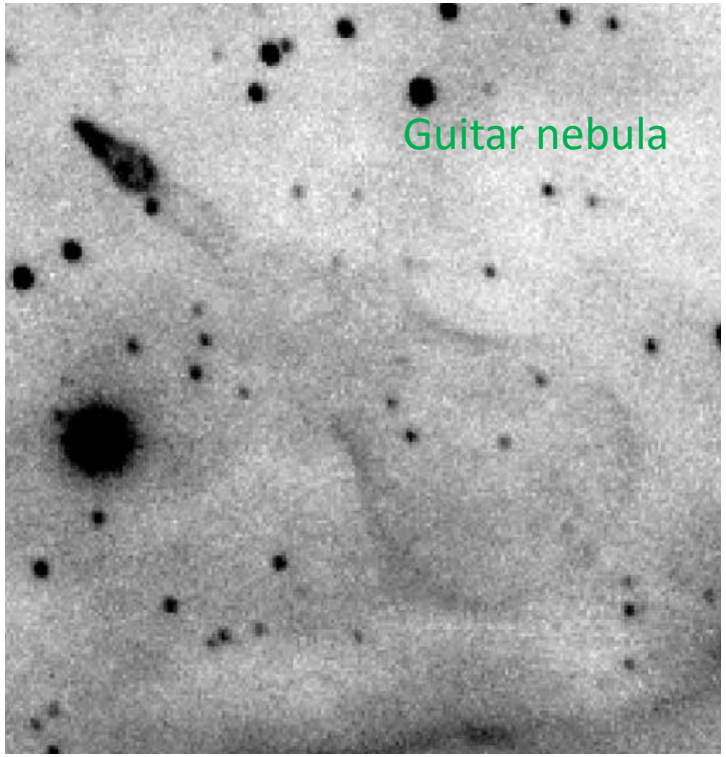

Chatterjee & Cordes 2002

(6) 脉冲星逃逸出遗迹壳层（发生的典型时标为若干万年），穿行于星际介质中，通常高度超声速；星风云受限于星际弓激波，呈彗星拖尾状。

(7) 最后阶段，脉冲星运行到低密度区域，不再超声速，能量输出微弱，裹在一个静态或缓慢膨胀的、为星际介质热压力束缚的相对论性气体腔中。

Supersonic PWN

#	Pulsar	Associated Object(s)	d kpc	$\log \dot{E}$ erg s^{-1}	$\log \tau$ yrs	B_{11} 10^{11} G	$v_\perp$ km s^{-1}
1	J0537–6910[a]	SNR N157B	49.7	38.68	3.69	9.25	...
2	B1951+32	SNR CTB 80	3	36.57	5.03	4.86	460
3	J1826–1256	HESS J1825–137	~ 3.9[b]	36.56	4.16	37	...
4	B1706-44	SNR G343.1–2.3	2.6	36.53	4.24	31.2	$\lesssim 100$
5	B1757–24	SNR G5.27–0.9, Duck PWN	3.8	36.41	4.19	40.4	198
6	J1747–2958	Mouse PWN	5	36.40	4.41	24.9	306 ± 43
7	J1135–6055	...	~ 2.8[b]	36.32	4.36	30.5	< 330
8	J1437–5959	SNR G315.9–0.0, Frying Pan PWN	8	36.15	5.06	7.37	~ 300
9	J1101–6101	Lighthouse Nebula, SNR G290.1–0.8	~ 7[b]	36.13	5.06	7.24	~ 2000
10	J1509–5850	...	4	35.71	5.19	9.14	$200 - 600$
11	B0906–49	...	1	35.69	5.05	12.9	~ 60
12	B1853+01[a]	SNR W44	3.3	35.63	4.31	75.5	400^{+114}_{-73}
13	B0740–28	...	2	35.28	5.2	16.9	275[c]
14	B1957+20	the Black Widow pulsar	1.73	35.20	9.18	0.002	~ 220
15	J0538+2817	SNR S147	1.39[P]	34.69	5.79	7.33	357^{+59}_{-43}
16	B0355+54	Mushroom PWN	1.04[P]	34.66	5.75	8.39	61^{+12}_{-9}
17	J0633+1746	Geminga PWN	0.25[P]	34.51	5.53	16.3	~ 200
18	J2030+4415	...	~ 1[b]	34.46	5.74	12.3	...
19	J1741–2054	...	0.3	33.97	5.59	26.8	155
20	J2124–3358	...	0.41	33.83	9.58	0.003	75[c]
21	J0357+3205	Morla PWN	0.5	33.77	5.73	24.3	~ 2000
22	J0437–4715	...	0.156[P]	33.74	9.2	0.006	104.7 ± 0.9
23	J2055+2539[a]	...	~ 0.6[b]	33.69	6.09	11.6	$\lesssim 2300$
24	B1929+10	...	0.36[P]	33.59	6.49	5.18	177^{+4}_{-5}
25	B2224+65	Guitar Nebula	1.88	33.07	6.05	26	1626
26	...	SNR IC443[a]	1.4	...	...	...	~ 250
27	...	SNR MSH 15–56, G326.3–1.8	4	...	...	...	100–400
28	...	G327.1–1.1, Snail PWN	7	...	...	...	~ 500

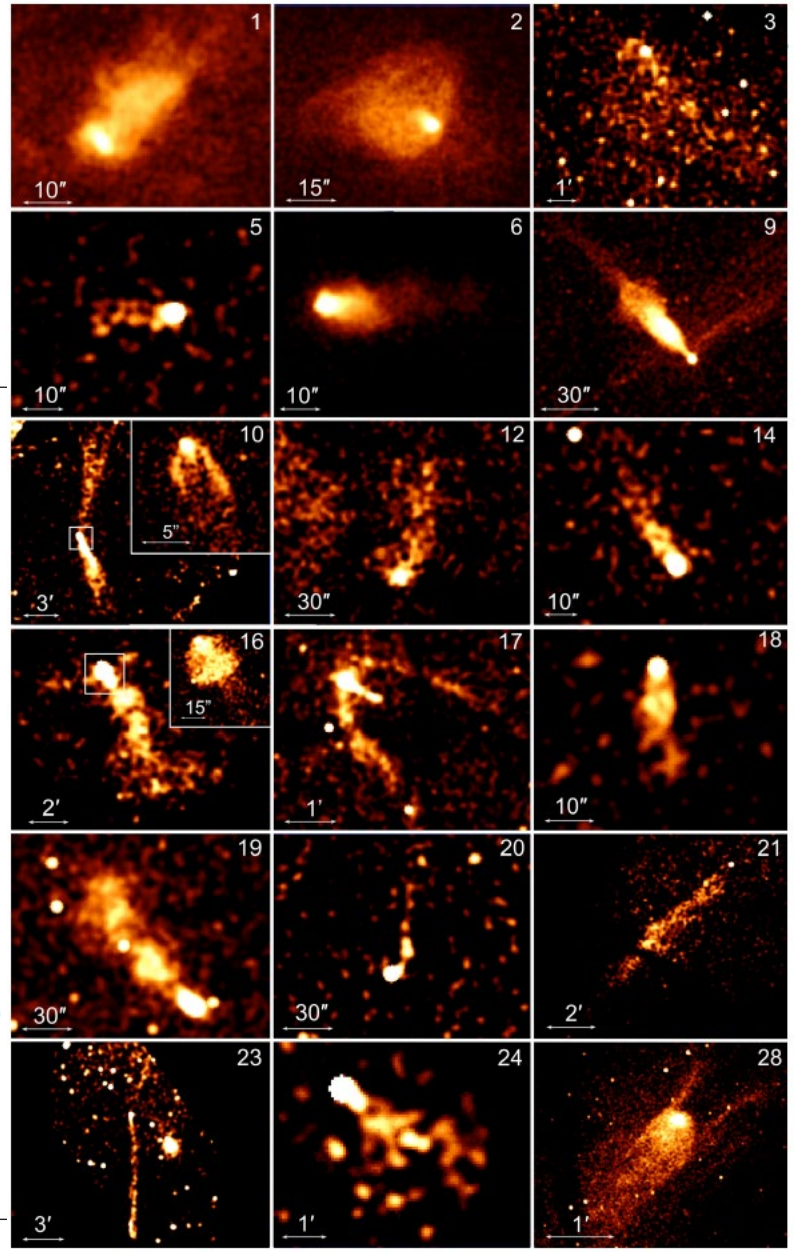

Kargaltsev+1708.00456

Pulsar (TeV) halos

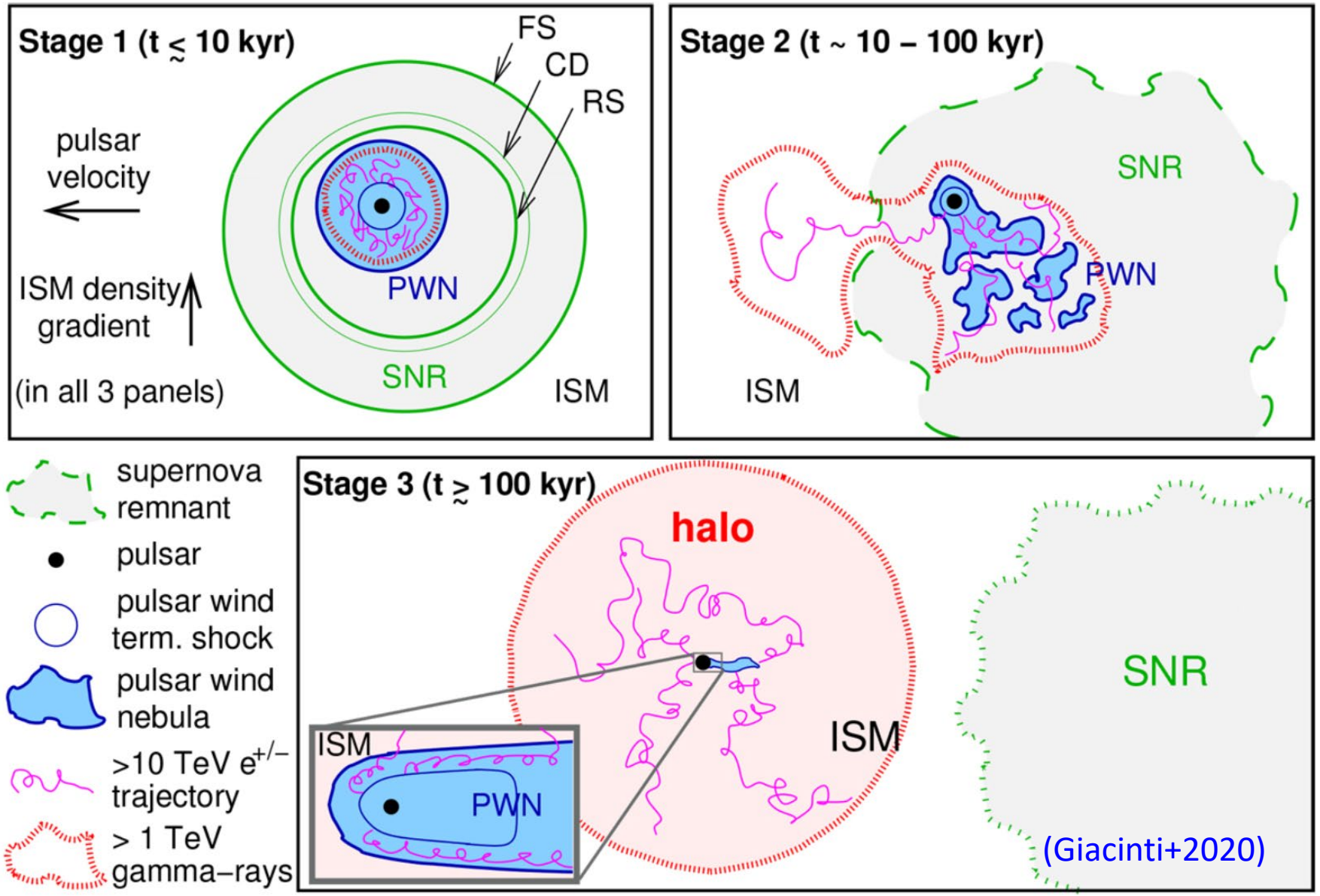

Type Ia SN progenitor: dubble or single degenerate ?

CSM in Kepler's SNR

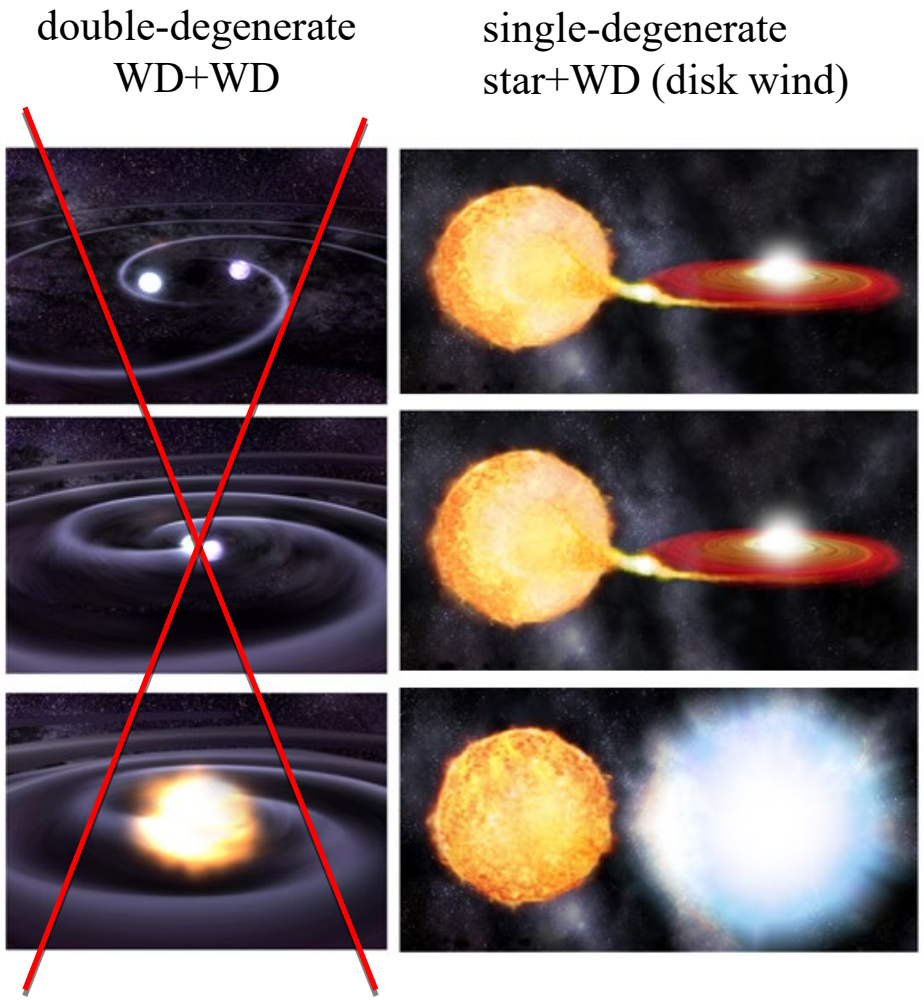

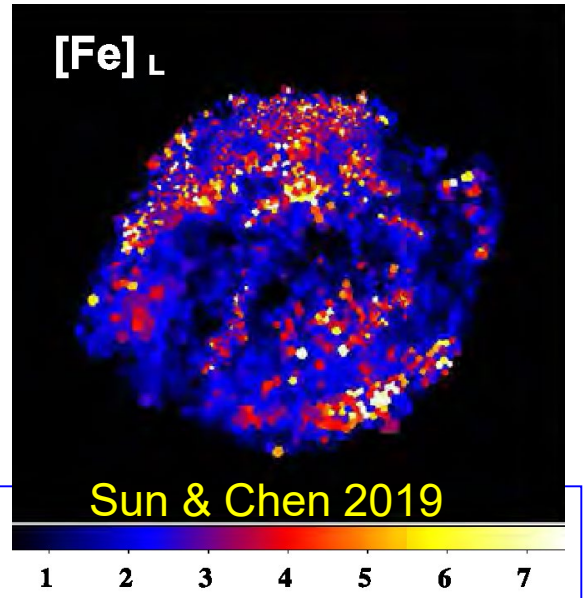

- CC SNR?
  N-rich, bow shocked like CSM
- Ia SNR?
- Location 590pc away from the Galactic plane
- **High [Fe] in X-rays, *conclusive* evidence**

- DD progenitor?
- No surving companion

- SD progenitor?
- **CSM-interaction**, suggesting AGB, core degenerate, subdwarf B star, etc.

Ia SNR Kepler

(Sun & Chen 2019)

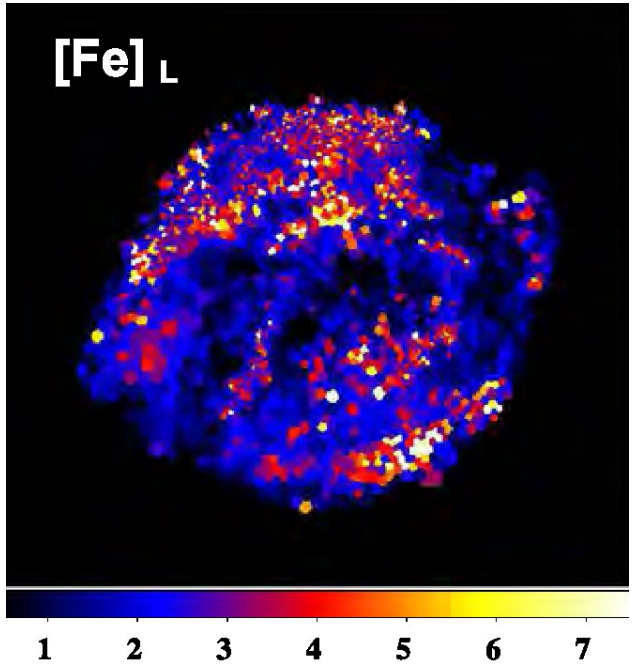

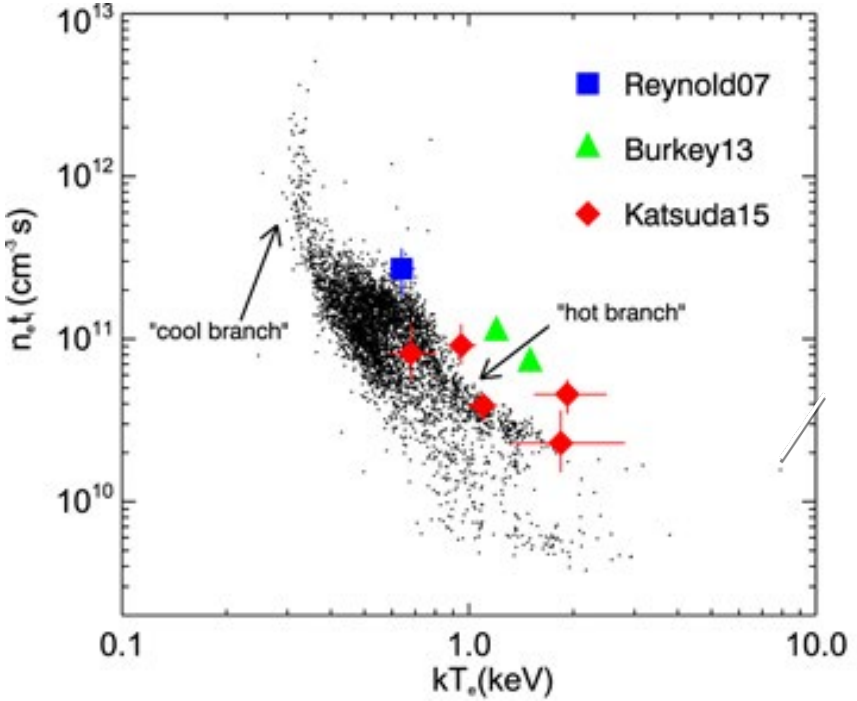

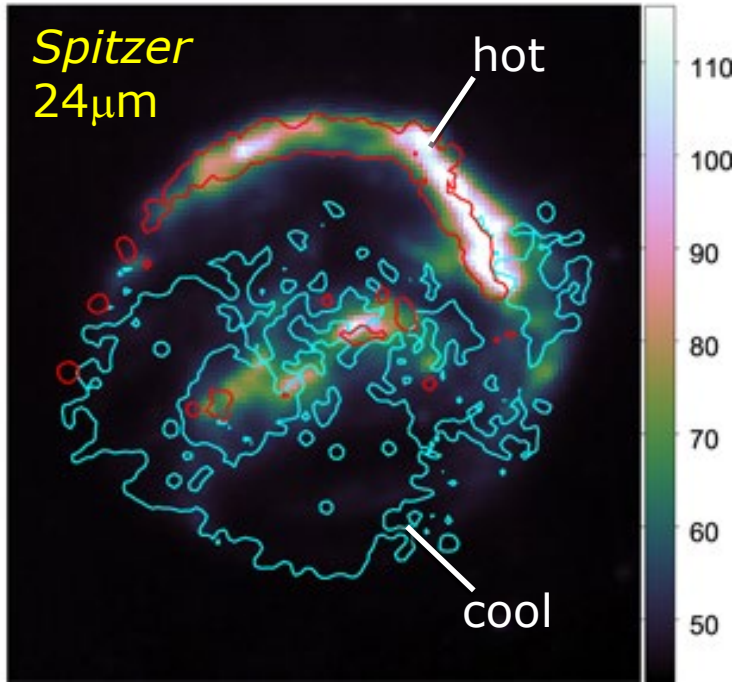

- Shocked CSM: $[O]/[Fe]_L \sim 0.77$, $[Mg]/[Fe]_L \sim 1.11$; mass~$1.4 M_\odot$ consistent with an AGB donor with $4 M_\odot$
- Shocked ejecta: $[O]/[Fe]_L \sim 0.31$, $[Mg]/[Fe]_L \sim 0.38$ compatible with “spherical delayed-detonation” model

G306.3-0.9: Calcium-rich Transient

(Weng et al. 2022)

Mass-weighted abundance ratios S/Si < Ar/Si < Ca/Si
compared with 20 SN models

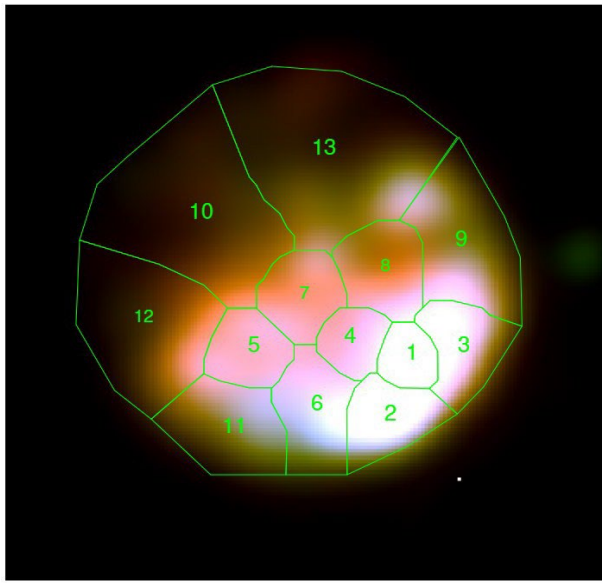

XMM-Newton pn image
red: 0.5-1.5 keV
green: 1.5-3.5 keV
blue: 3.5-7.0 keV
.

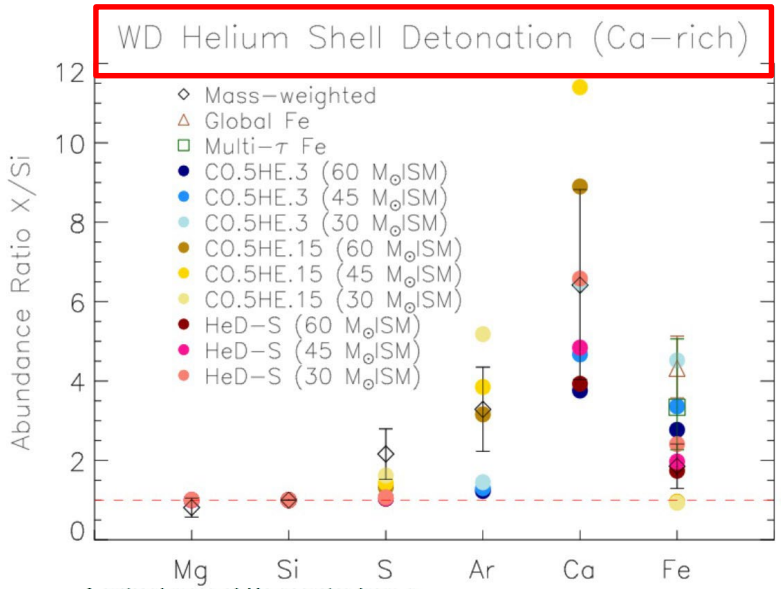

A critical mass of He accretes from a companion. The helium ignites and detonates. This may set off a secondary detonation of the carbon

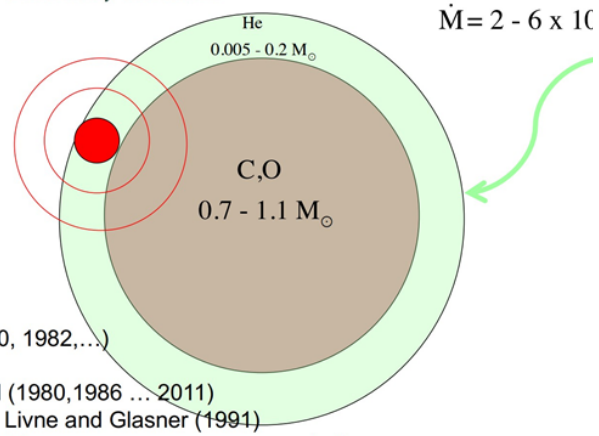

Nomoto (1980, 1982,...)
Taam (1980)
Woosley et al (1980,1986 ... 2011)
Livne (1990); Livne and Glasner (1991)
Fink et al (2007)
Sim et al (2010) Shen and Moore (2014ab) Shen et al (2017)
and others

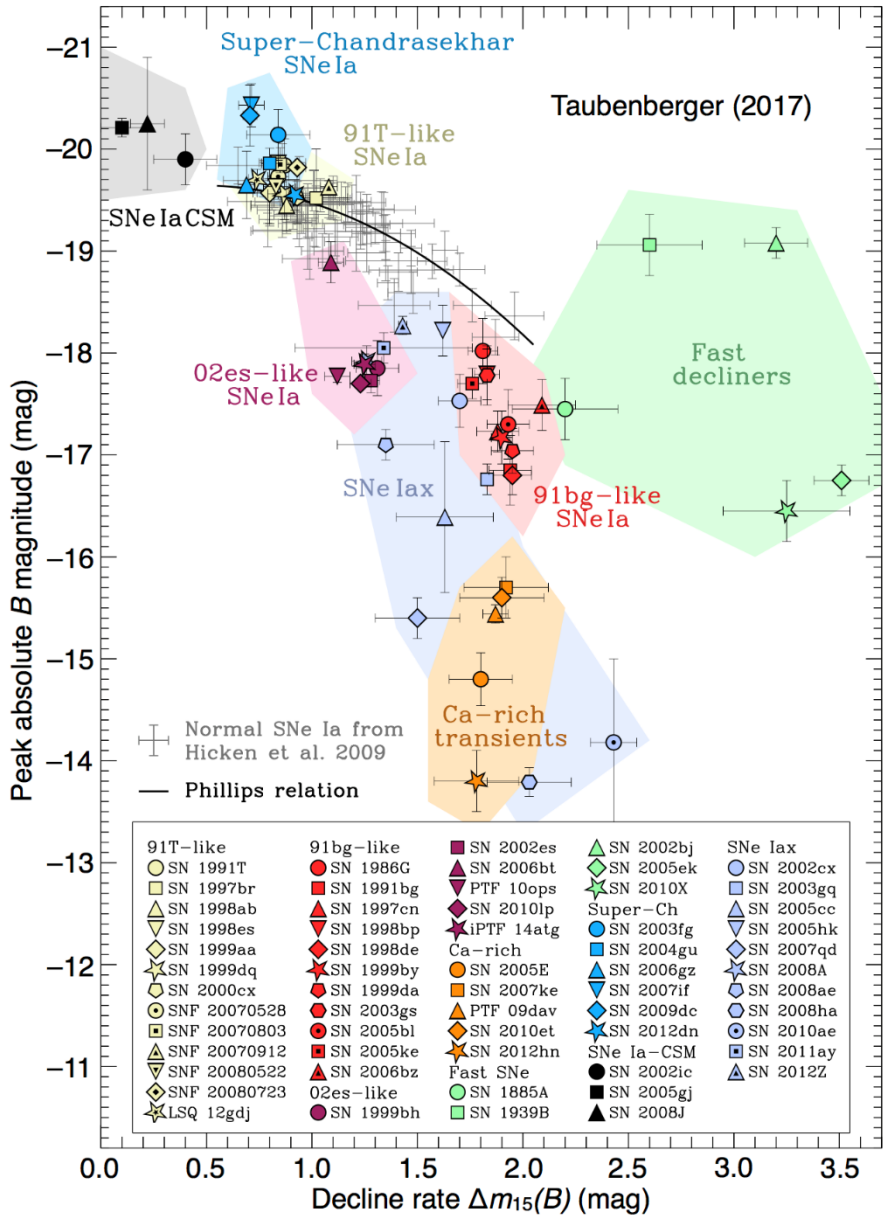

Possible Mechanisms for thermal composites

Candidate mechanisms for thermal composites SNRs:

1. Rim radiative cooling
(interior still hot to emit X-rays)
2. Thermal conduction
(to distribute enough gas near the center)
3. Cloud evaporation
(gas evaporated from dense cloudlets)
4. Projection effect
(projection of dense gas shock)
5. Metal line emission
(dust destruction & ejecta enrichment)
…… ?
*. Shock reflected inward !
(by the wind-cavity wall)

- Models of Radiative Rim & Thermal Conduction

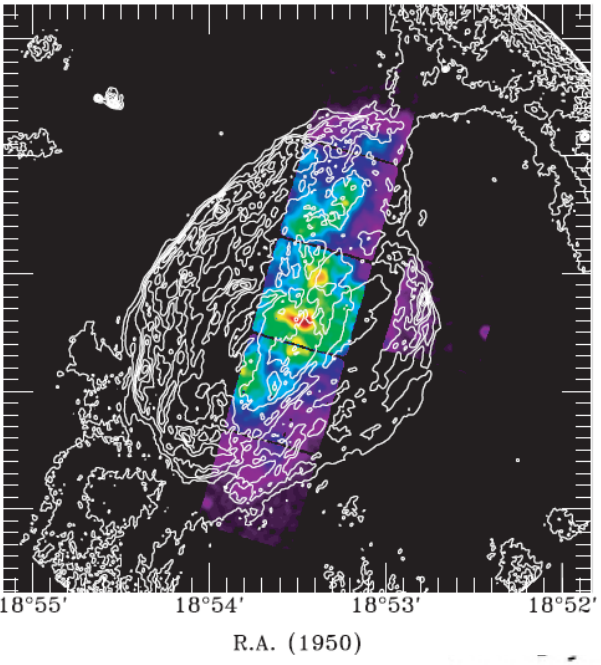

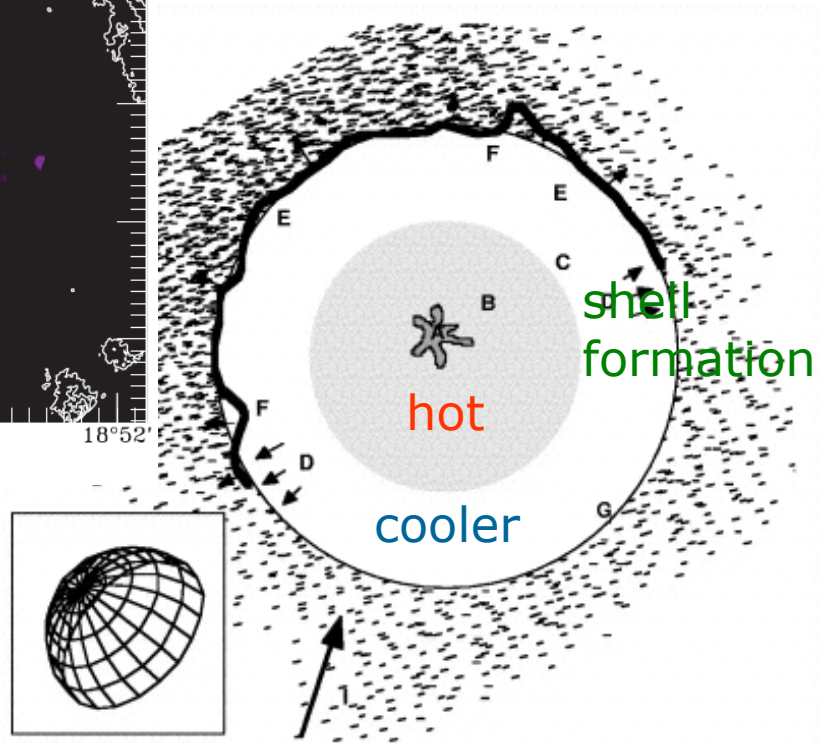

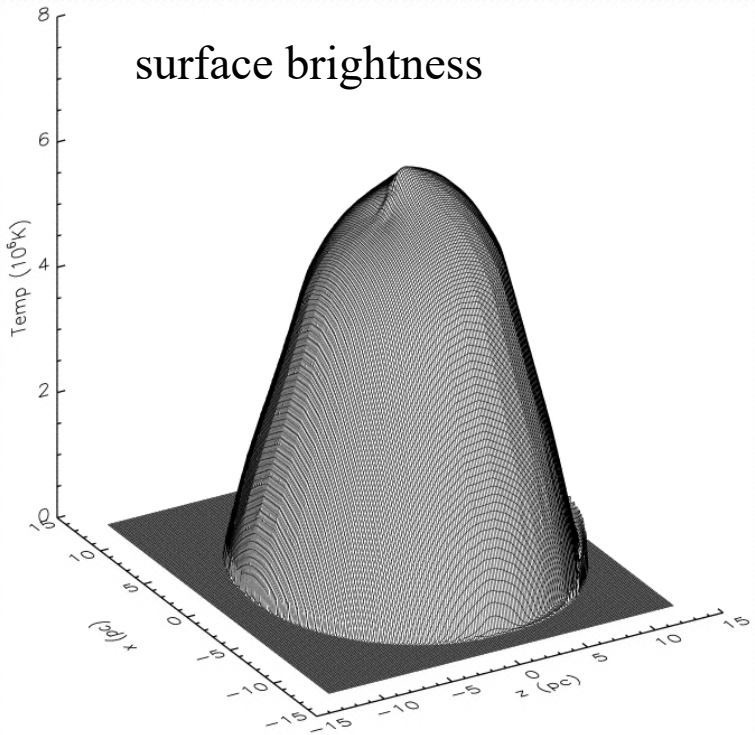

(Cox et al. 1999, Shelton et al. 1999)

- ❑ SNR old, radiative shell formation, rim faint in X-rays
- ❑ Thermal conduction smoothes out *T* gradient, increases central ρ (seems **applicable to W44**)
- ❑ *difficult for uniform T distribution (Kes 79, 3C391, etc.)*

- Model of Cloudlet Evaporation

Evaporation of clumpy ISM (White & Long 1991)

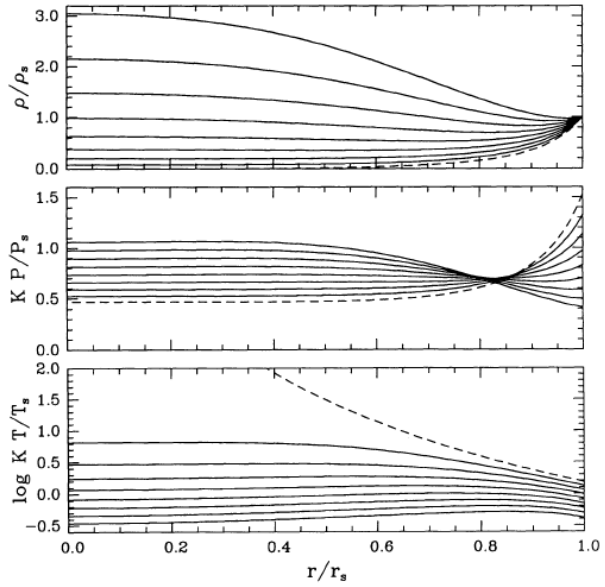

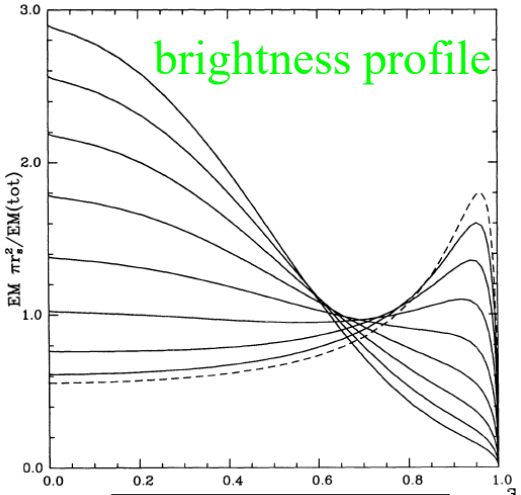

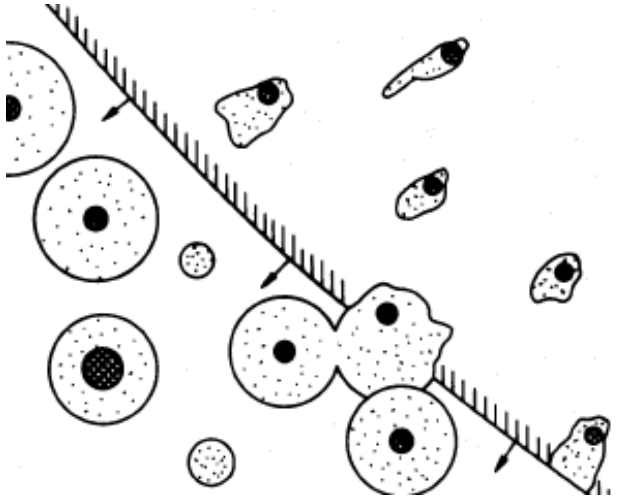

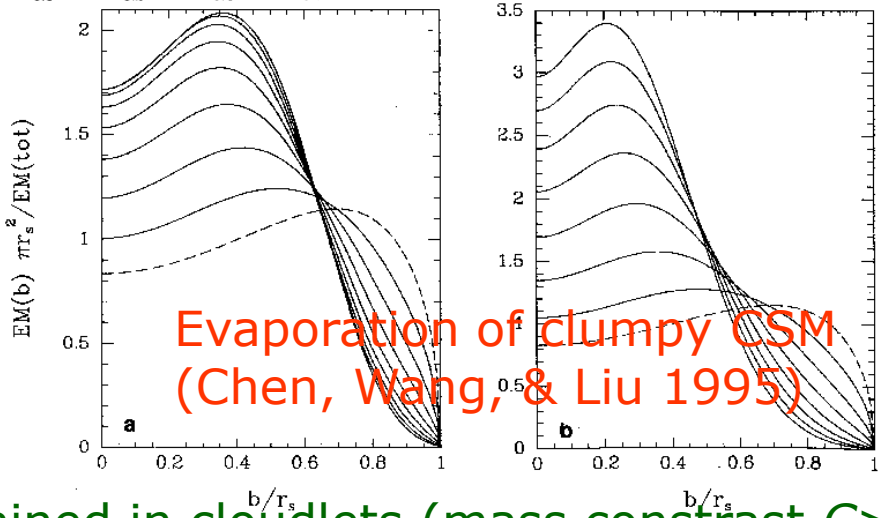

Evaporation of clumpy CSM (Chen, Wang, & Liu 1995)

n_H (cm^{-3})/$f^{-1/2}d_8^{1/2}$

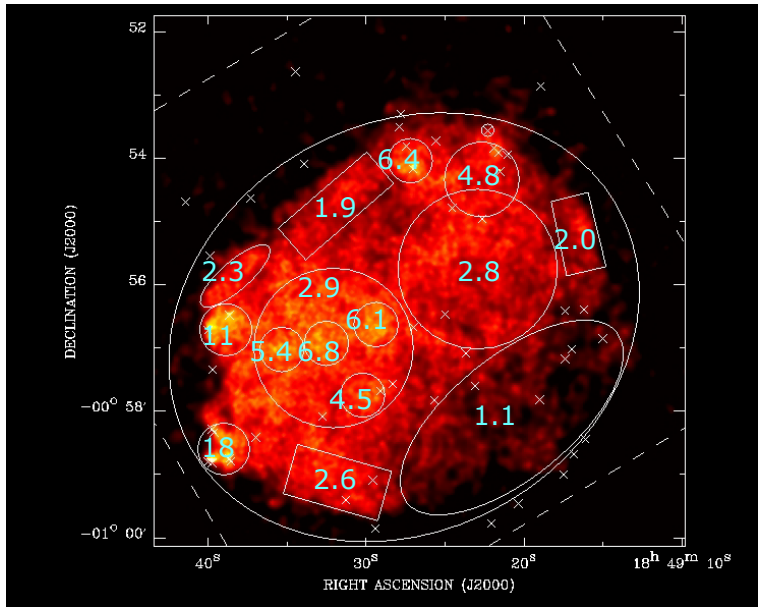

3C391 (Chen+ 2004)

- Mass of ISM mostly contained in cloudlets (mass constrast $C>1$)
- Evaporated gas lowers central T, increases central ρ (T and ρ almost uniform!)
- *difficult for SNRs with equilibrium ionization (W44, W28, etc.)*

- Shock reflection

(Chen et al. 2008, ApJ, 676, 1040)

What if an SNR impacts on a cavity wall?

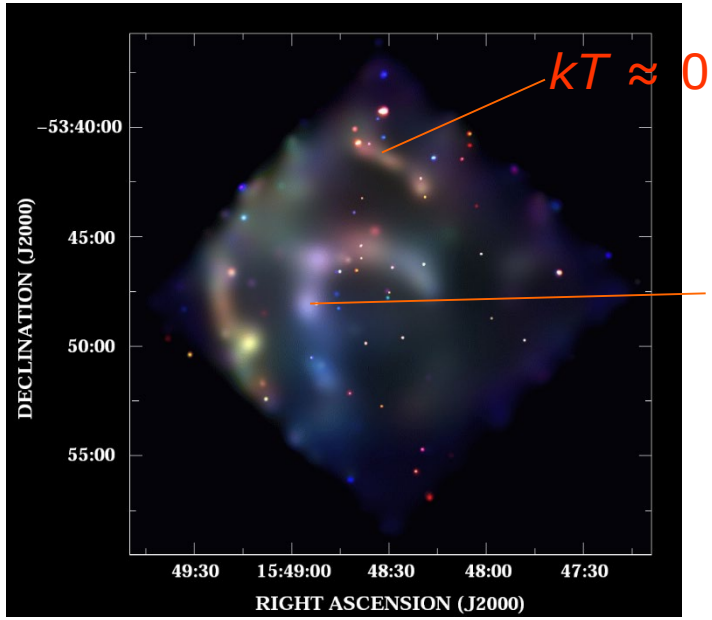

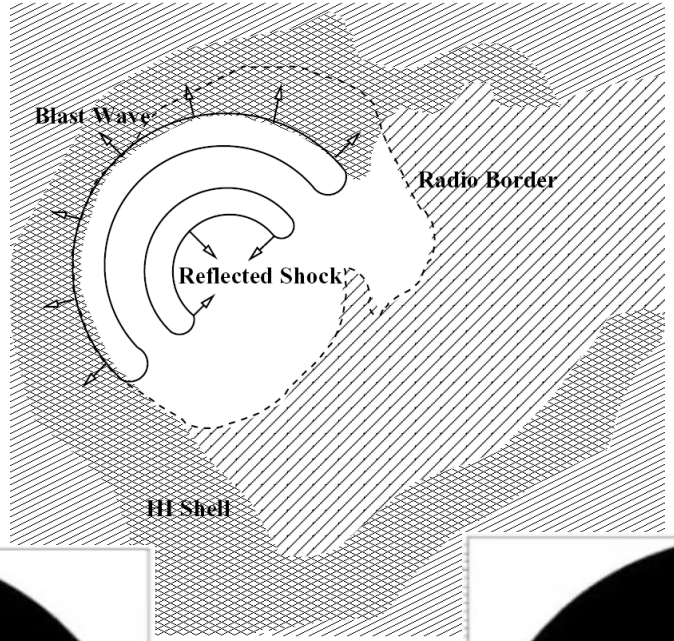

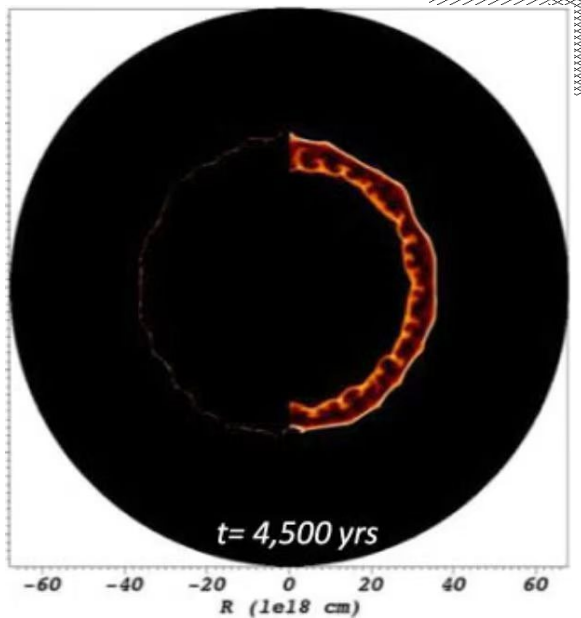

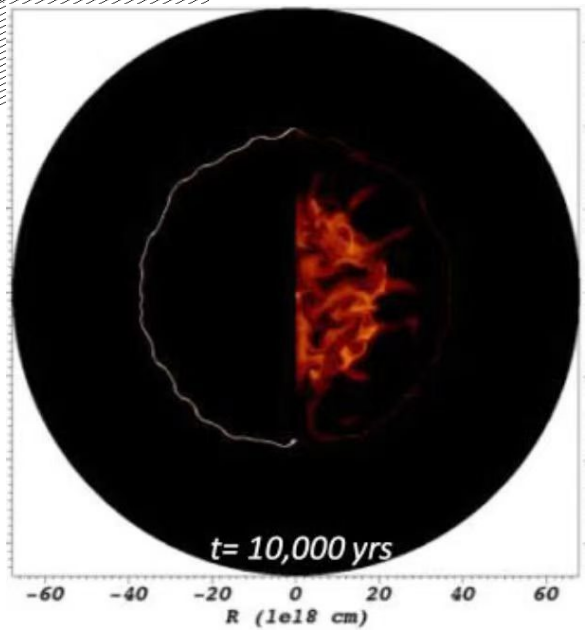

(Chiotellis et al. 2024)

A subclass of TC SNRs:
enhanced-abundance / ejecta-dominated

(Lazendic & Slane 2006) (Pannuti+ 2014)

- 25-30 (67%-81%) among 36-37 known TC SNRs: $z > 1$
- ~14 (50%) of them in the subclass associated with MCs

Questions:

- Why are these X-ray emitting gas evolving in MCs ejecta dominated? (Not mixed / diluted?)
- Any relation to the physical nature of TC SNRs?

Sub-class TC: Ejecta-dominance

MOPRA

Most of the subclass TC SNRs are in cavities!

SNR Kes 41

(Zhang, Chen+ 15)

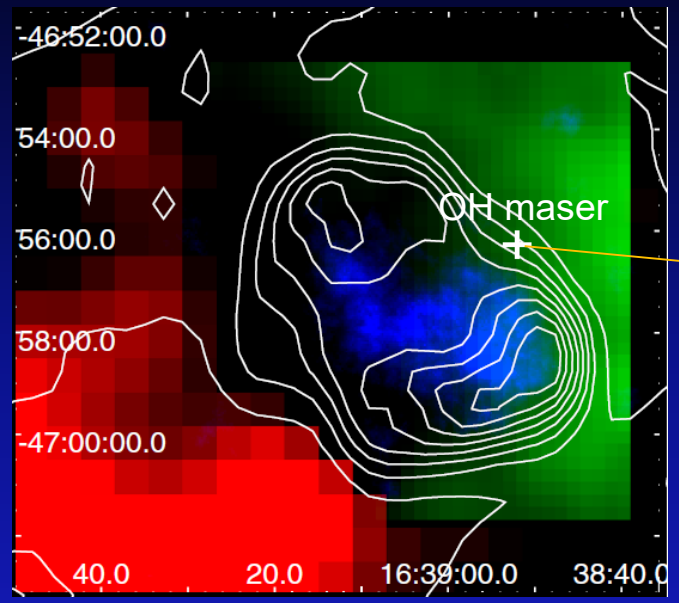

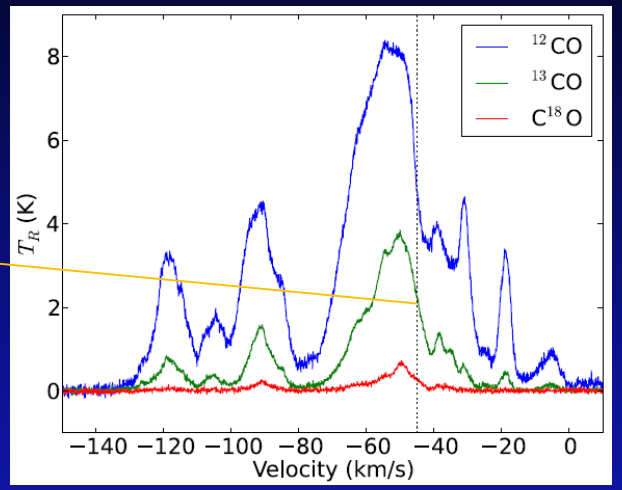

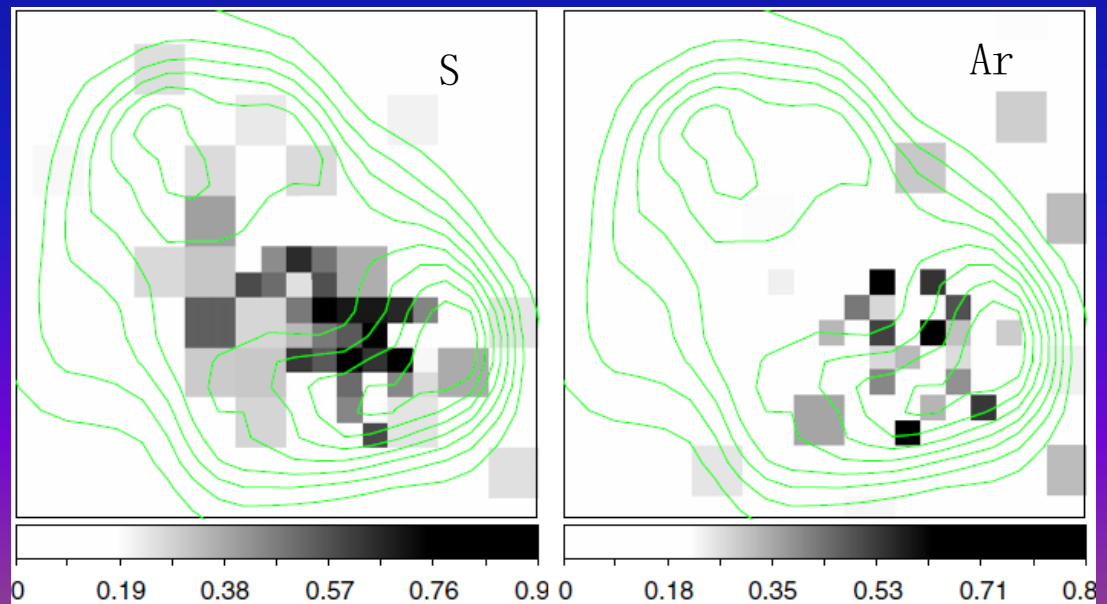

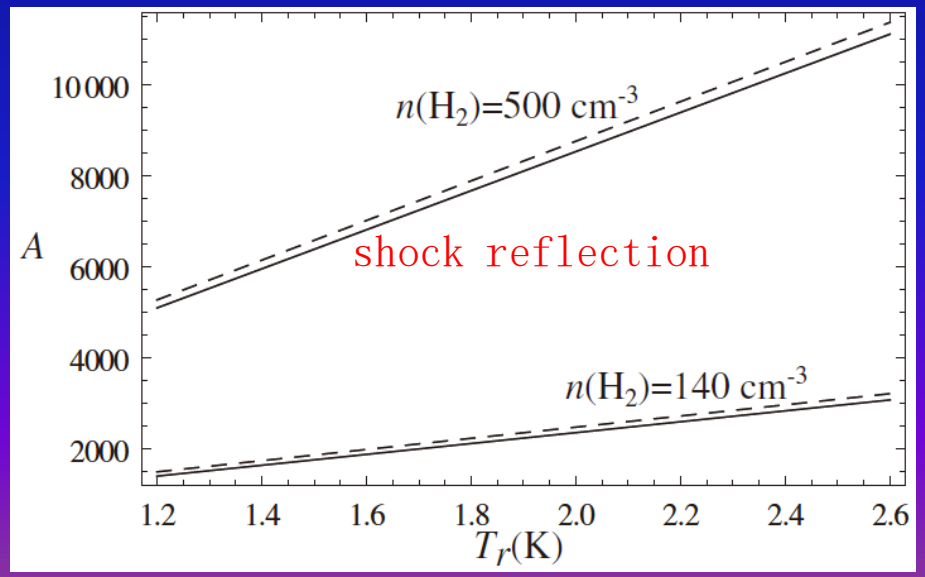

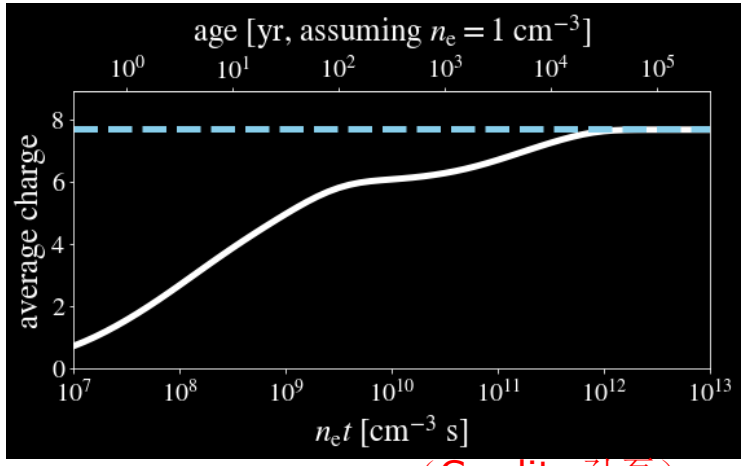

（Credit: 孙磊）

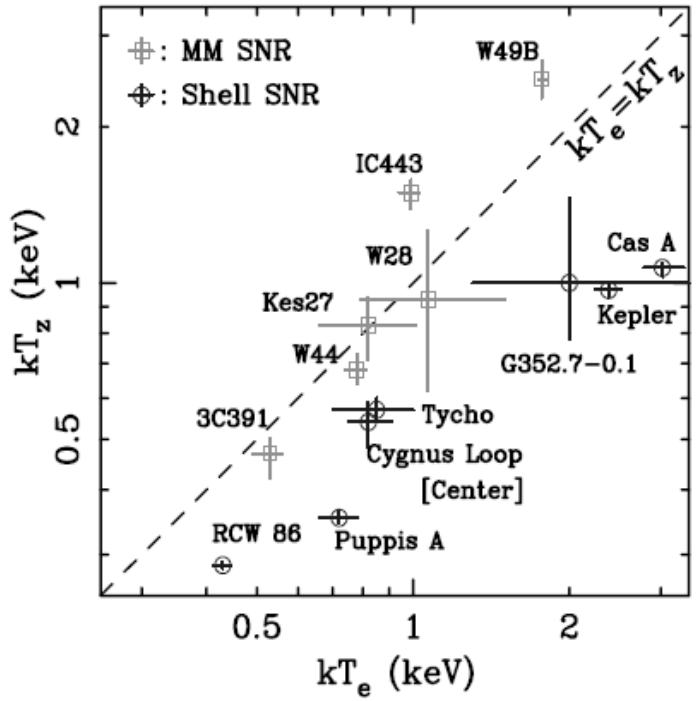

TC (MM): $kT_z > kT_e$
Shell: $kT_z < kT_e$

Unified NEI Scenario?

Kawasaki et al.'s (2005)

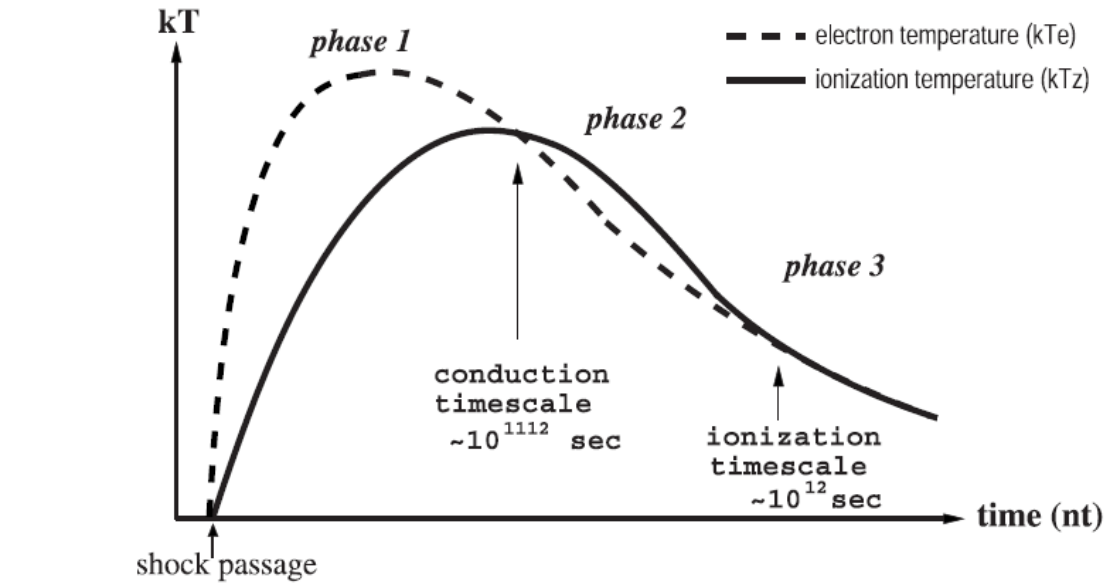

Ionization state	underionized	--→ overionized --→	equilibrium
X-ray morphology	shell-like	----→	center-filled
evolutionary phase	Sedov phase	----→	conduction phase

Possible origins of recombining plasmas

Decrease in kT_e (electron cooling)

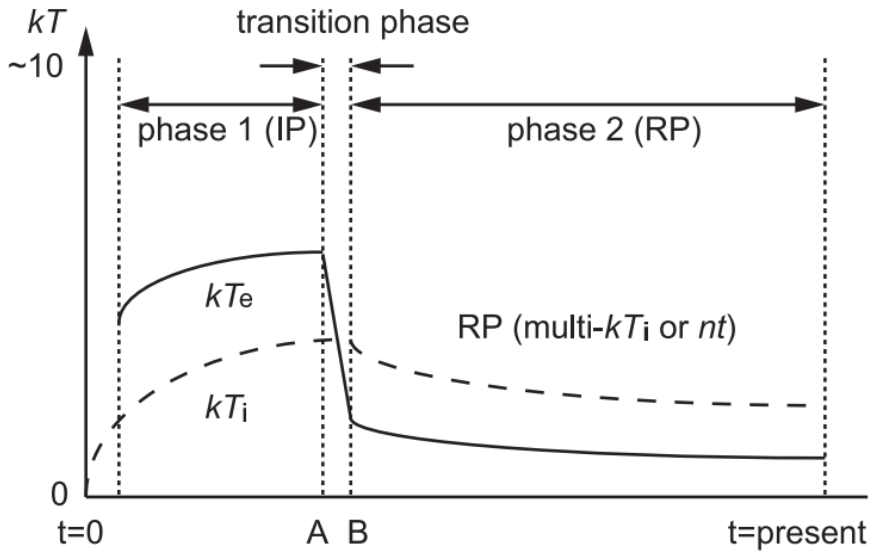

- Adiabatic cooling (e.g., Itoh & Masai 1989)
- Thermal conduction (e.g., Kawasaki et al. 2002; Zhou et al. 2011; Zhang et al. 2019)

Increase in kT_i (extra ionization)

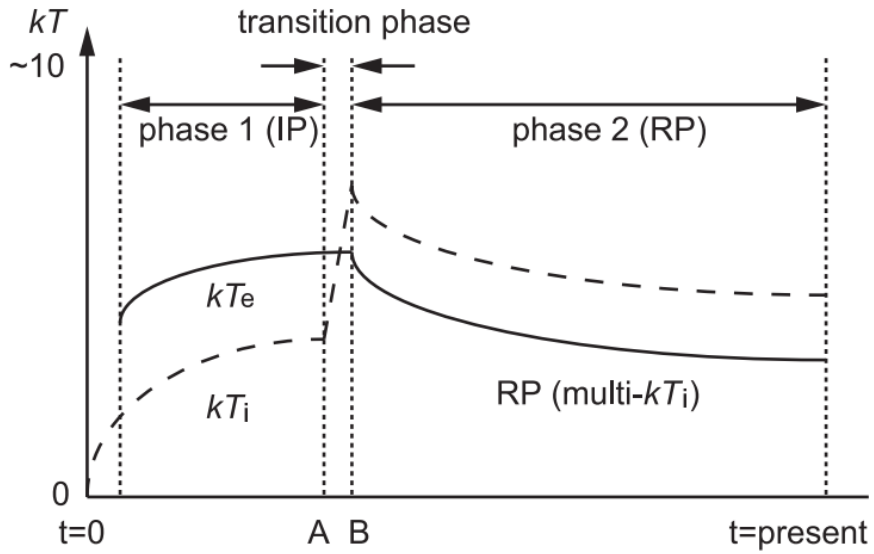

- Suprathermal electrons (e.g., Ohnishi et al. 2011)
- High-energy photons (e.g., Kawasaki et al. 2002)
- Low-energy cosmic rays (LECRs, e.g., Yamauchi et al. 2021)

1st *NEI* simulation for thermal composites

Zhang+19,ApJ

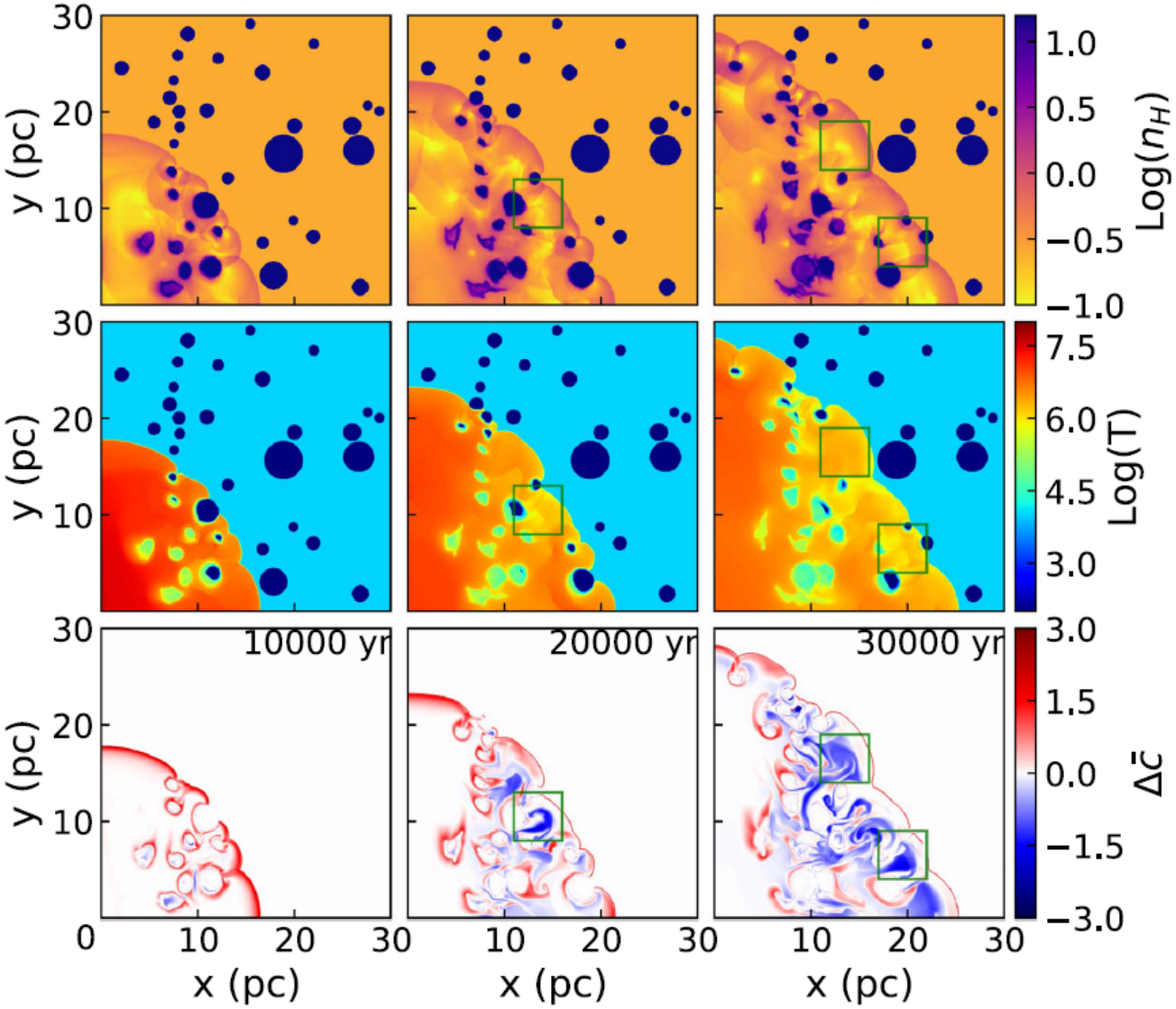

Red: ionizing
Blue: recombining

- classic conduction
- evaporation
- expansion

EP-FXT: large FOV and effective area

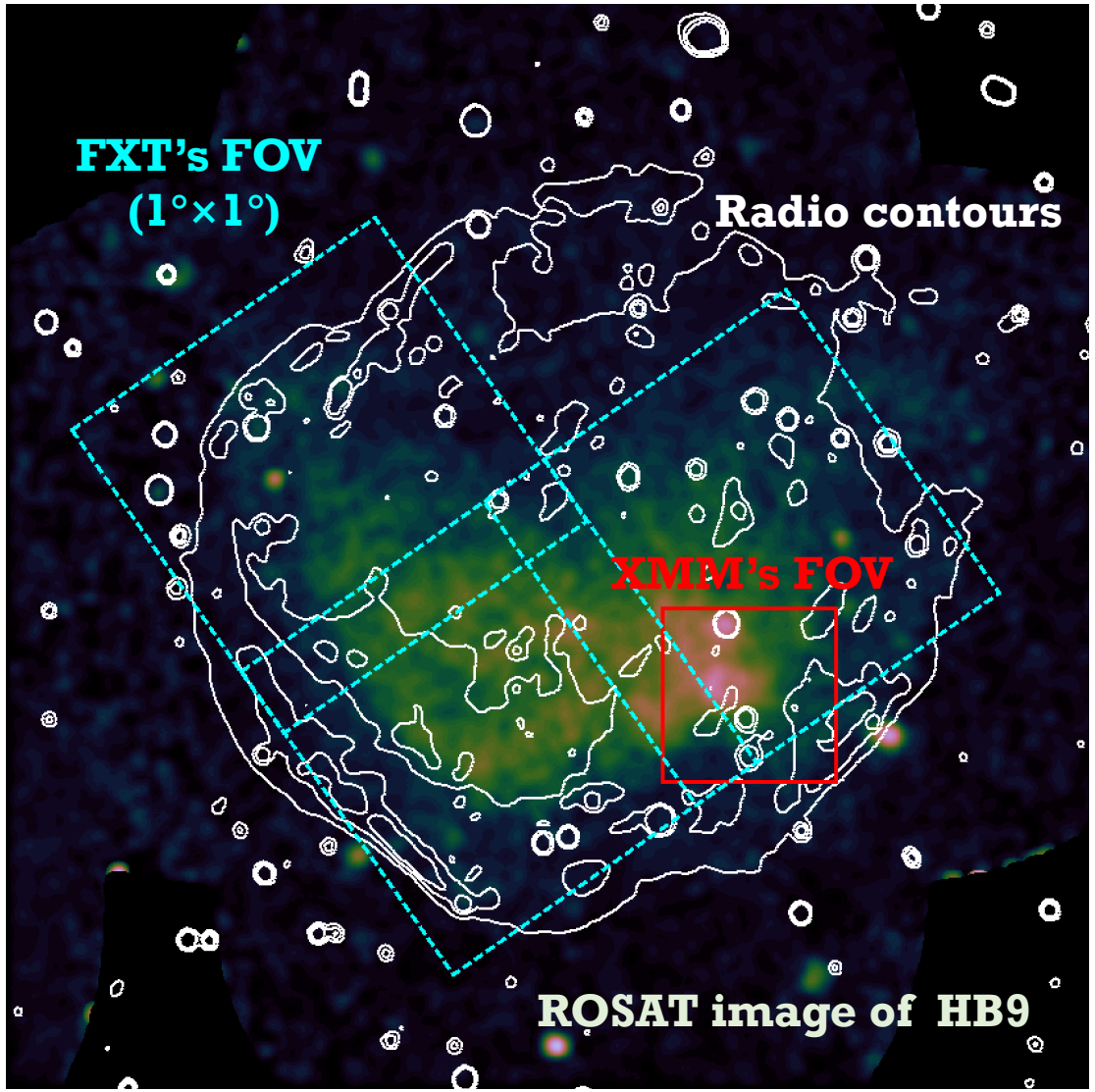

Simulated 25 ks FXT spectrum of a subregion of HB 9

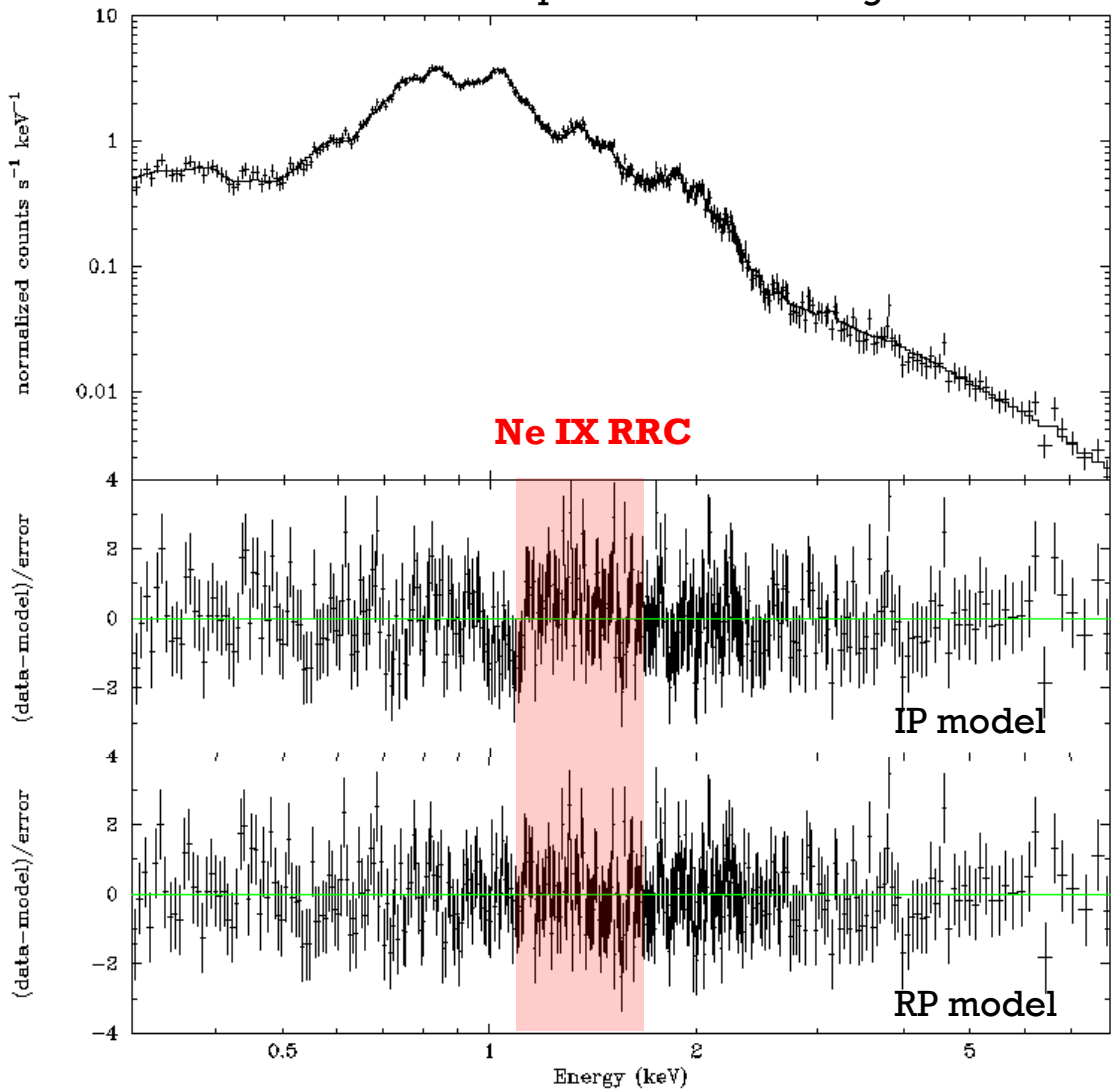

EP proposal (Lei Sun, Hanxiao Chen, Yang Chen)

祝同学们暑假快乐！